BARC
NEWSLETTER

Ahmedabad City Sludge Hygienisation Facility

Radiation Source

CONTENTS

Development of 1.5 kW, 5 kHz IGBT based Induction Heating Inverter for Laboratory Level Heating Applications for Scientific and Material Studies

B.M. Barapatre and J.S. Pakhare
Electronics & Instrumentation Group

Developed Induction Heating Inverter, although was a PRIS G target for ATSS, will be useful in laboratory level heating applications in the field of scientific and material studies and various material processes. Inverter is rated for 1.5 kW at 5 kHz output frequency. Heating of stainless steel pipe, assumed as a susceptor/crucible (70mm dia, 150 mm long, 3mm thick) with 50 mm heating zone, is achieved up to 800°C.
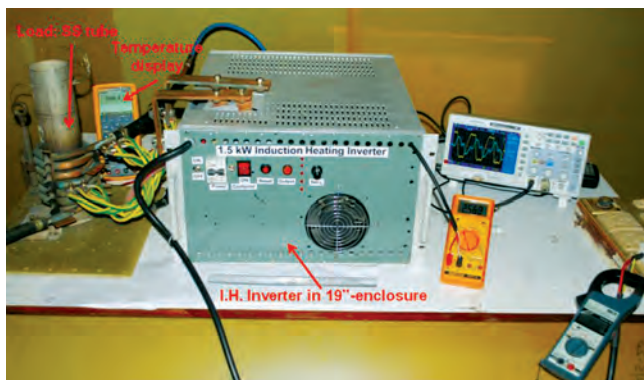
Fig. 1: 1.5kW Induction Heating Inverter assembled in standard 19-inch enclosure.

Design is based on half bridge series resonant inverter topology. This topology works under open circuit load as well as short circuit load. This is designed with standard control &

protections requirements of power electronics system. All semiconductors and electromagnetic components of this inverter are force air cooled; only output bus-bar and load coil is water-cooled.

The constant on-time variable frequency type controller has been selected for operation of the inverter. It always ensures zero current-voltage switching of the semiconductor devices resulting zero switching losses throughout the operating frequency range. This makes them highly efficient, low in harmonic distortion and low in EMI. IGBTs are utilized instead of traditional SCRs as switching device for this application.

In order to control the output power from minimum to maximum, the output frequency is varied from 2 kHz to 5 kHz.

With 1.5kW power at the output, susceptor area covered under the load coil gets heated up to 800°C in 6 minutes. The K-type thermocouple is used to measure temperature and it is displayed on 4½ digit display. Test results are shown below in Figs. 2, 3 & 4.

(a)

(b)

Fig. 2: side view (a) and top view (b) of Susceptor/Crucible at ~ 800°C
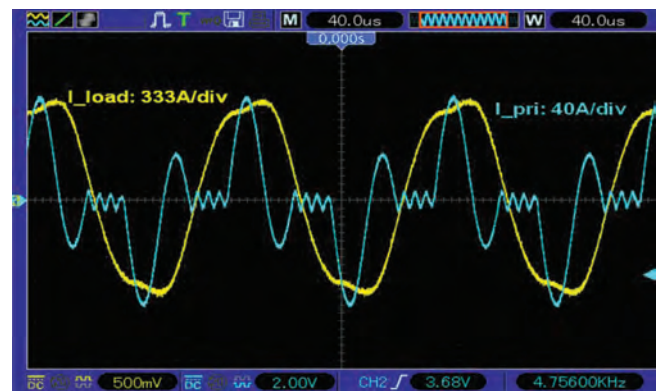
Fig. 3: Load Current and Voltage at 4.8kHz
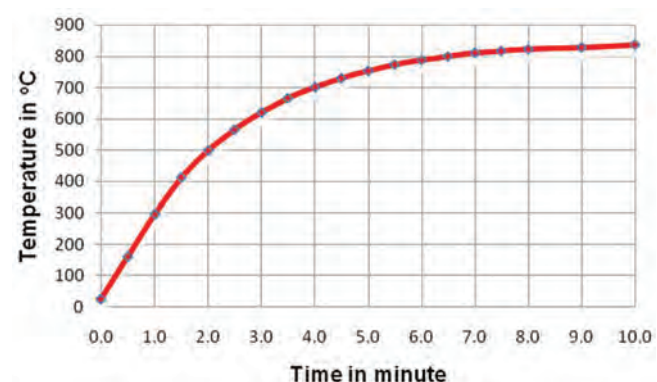
Fig. 4: Temp in °C vs time in minute

Brief Communication

A Biodegradable, Non Toxic, Inexpensive Superabsorbent for Effective Removal of Underwater Heavy Oil Using Radiation Technology

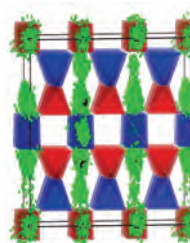**Atanu Jha, Subhendu Ray Chowdhury, B.S Tomar and K.S.S. Sarma**
Isotope and Radiation Application Division, Radiochemistry and Isotope Group

With the increase of offshore drilling of oil, production and transportation, the chances of oil spillage has enormously increased.[1] Materials with selective wettability, that is superhydrophobicity and superoleophilicity, or superhydrophilicity and superoleophobicity, can be used to separate the oil/water mixture.[2,3] In the last few years development of materials with special wettability for oil-water separation has received tremendous research and industrial interest. But easy and scalable methods for efficient absorbent preparation, separator with capability to separate oil from layered and emulsified oil-water mixture is not sufficient as per demand. Moreover, another severe problem is the removal of heavy oil from the underwater environment[4].

In this work, we have modified a gauze cotton (hydrophilic and oleophilic in nature) by gamma radiation assisted long chain hydrocarbon grafting. Upon modification the cotton turns its surface wettability by 360°, from superhydrophilic (water contact angle $< 10^{o}$) to superhydrophobic (water CA more than 158°) without sacrificing its liking towards oil (Fig. 1). In water environment it forms a unique interface around it, which functions like a 'no water zone' and that remains underwater for several days without allowing any water to get in. In the underwater environment it picks up heavy oil very fast and efficiently (25 to 35 times of its weight depending on oil density), when it comes into the contact of oil (Fig. 3). 1gm of cotton takes around 30gm of oil in 10 sec thereby attaining a complete saturation, when the system is layered (Fig. 4). For emulsion it takes 10-20 min to remove oil from oil/water mixtures (Fig. 5). The absorbed oil can be completely recollected by centrifuging the absorbent at 700 rpm (Fig. 6) and the same piece of absorbent can be repetitively used for more than 50 times for the same purpose without compromising with its mechanical & special wetting properties. Oil absorption capacity of the cotton has been studied by varying different kinds of oils namely, motor oil, diesel, edible oil (mustard oil), toluene, chloroform, dichloromethane etc.

More interestingly, the modified cotton is found chemically robust in various pH environments (Fig. 7). We have developed this material in a large scale. Thus, this biodegradable, non toxic, inexpensive, robust (chemically and mechanically) superabsorbent can be used as an efficient and fast underwater heavy oil remover. It can be extensively used for removal of oil from any part of water starting from surface to the bottom-most layer.
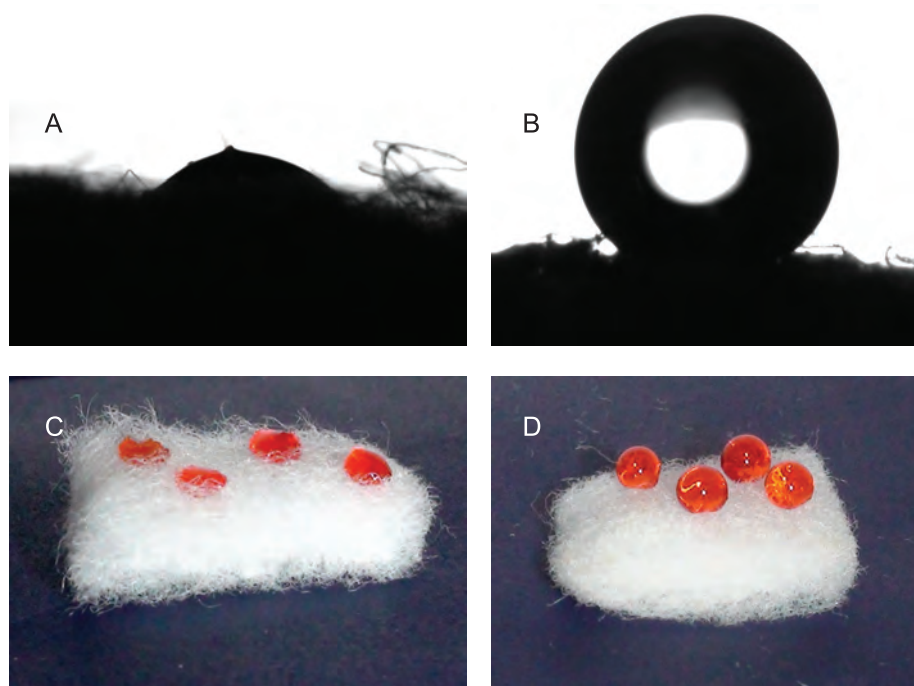
Fig. 1: Contact angle and beading of dyed liquid water on both the pure cotton (A,C) and grafted cotton (B-D) [superhydrophilicity and superhydrophobicity
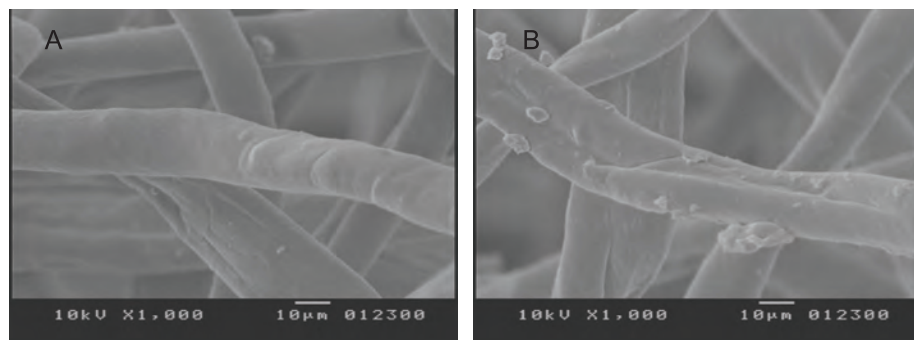
Fig. 2: SEM Images of (A) pure cotton and (B) grafted cotton
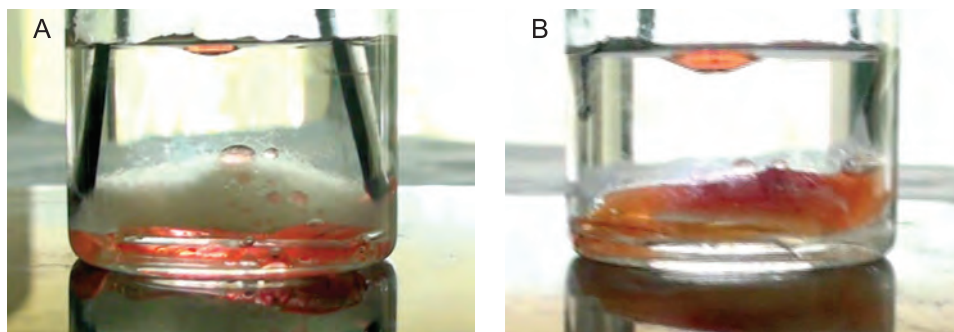
Fig. 3: Underwater (A) oleophobicity of pure cotton and (B) oleophilicity and rapid oil absorption by modified cotton
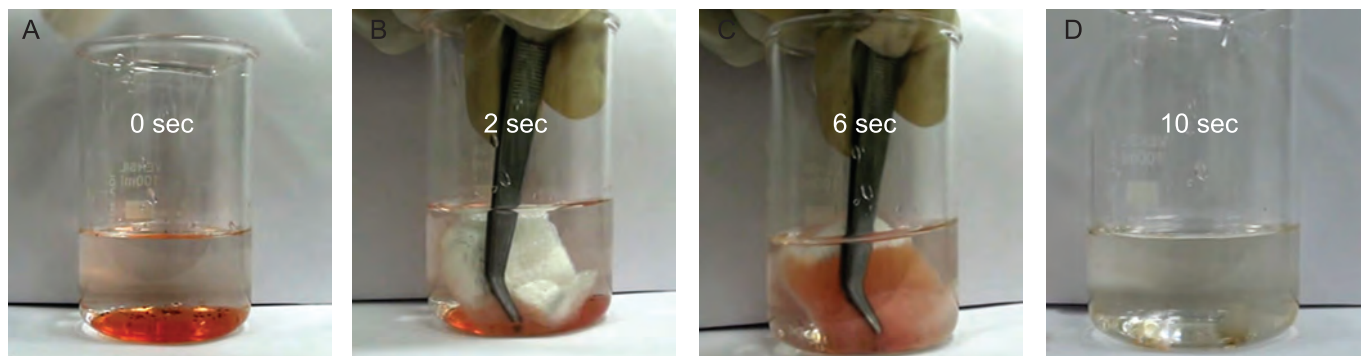
Fig. 4: Diagrammatic representation of layered oil (red dyed) separation from oil-water mixture (A-D)
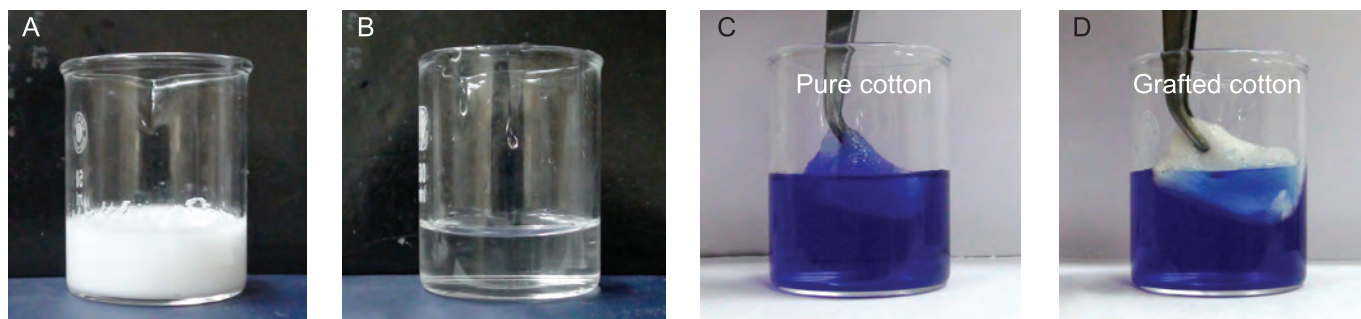
Fig. 5: A-B: Oil-water emulsion separation and C-D: underwater superhydrophilicity of pure cotton and superhydrophobicity of grafted cotton [blue solution is crystal violet added water]
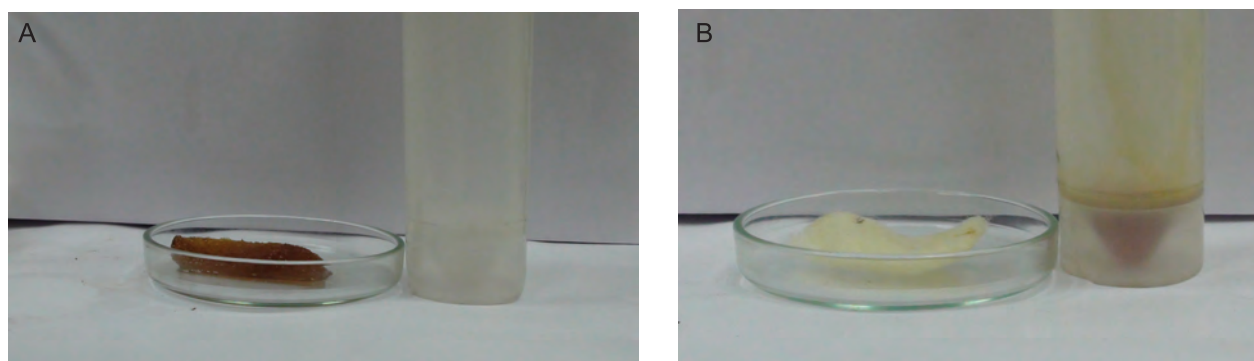
Fig. 6: Recollection of absorbed oil by centrifugation at 700 rpm (A,B) in 1 min
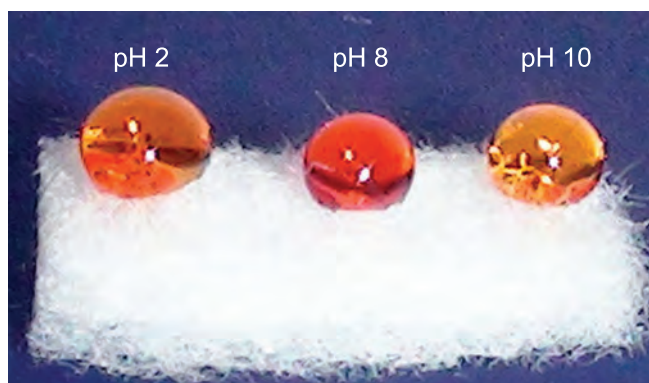
Fig. 7: Beading of acidic, sea water & alkaline droplets on modified cotton (chemical robustness)

References:

1. Peterson, C. H.; et. Al B. Science 2003, 302, 2082-2086.

2. Chu , Z. ; Feng , Y.; Seeger, S. Angew. Chem. Int. Ed. 2015 , 54,2328-2338.

3. Ma, Q.; Cheng, H.; Fane, AG.;Wang, R.; Zhang, H. Small, 2016, 12, 2186-2202.

4. Yong, J.; Chen, F.; Yang, Q.; Bian, H.; Du, G. Advanced materials interfaces, 2016, 3, 1500650-1500657

Atmospheric Pressure Plasma Jet for Radioactive Decontamination: A Glove Box Based Study

R. Kar, A. Bute, N. Chand and S. Sinha
Laser & Plasma Surface Processing Section
D.S. Patil
Laser & Plasma Technology Division
Romesh Chandra
Accelerators and Pulsed Power Division
P. Jagasia and P.S. Dhami
Fuel Reprocessing Division

We have designed and developed an APPJ device for solid nuclear waste removal. Synthetic Plutonium samples were used as radioactive source and with the help of this device upto 92% decontamination was achieved under optimized condition inside glove box. A scaled up multi-electrode model APPJ reduced the operational time by 50% in comparison to single electrode device. Optimized Argon flow rate of 6 LPM ensured stable plasma jet and high decontamination. Portability, operational ease, high decontamination efficiency and very low secondary waste generation makes this technique a potential alternative to radioactive decontamination in nuclear waste management.

Introduction:

Volume reduction of radioactive waste is of paramount importance in nuclear energy program. Many researchers are working towards development of innovative processes for this purpose [1]. Since early nineties few research groups have reported plasma etching as an alternate option for decontamination in solid nuclear waste [2-4]. Plasma works at least 200 times faster than the conventional processes and atmospheric pressure plasma jet (APPJ) could be a potential alternative for radioactive decontamination due to their high chemical conversion rate, favorable economics, ease of operation, small size and low operational costs [2].

In spite of these advantages, there exist few recent reports on plasma based decontamination. Hence, our work focuses on a detailed investigation of this technique when applied to a Pu contaminated α samples. In this study we have developed a prototype APPJ and installed it inside a glove box for solid radioactive waste removal. Based on its success a scaled up multi-electrode plasma device was designed and employed inside a glove box. Both of these devices under optimized condition could eliminate radioactive wastes and the scaled up device reduced the operation time by as much as 50%.

Design of Microwave APPJ Device:

To match the characteristic impedance of the device with that of the co-axial cable (50 Ohm) [5], we use the below equation.

$$Z_0 \approx (138/\sqrt{\varepsilon_r}) \log_{10}(D/d) \qquad (1)$$

Where ε_r is the relative permittivity, D is inner diameter of the outer tube and d is diameter of the inner rod (Figure 1(a)). D and d were fixed as 140 and 6.35 mm respectively making $Z_0 \sim 47.4$ Ohm. Photograph of the APPJ device is shown in Fig. 1.
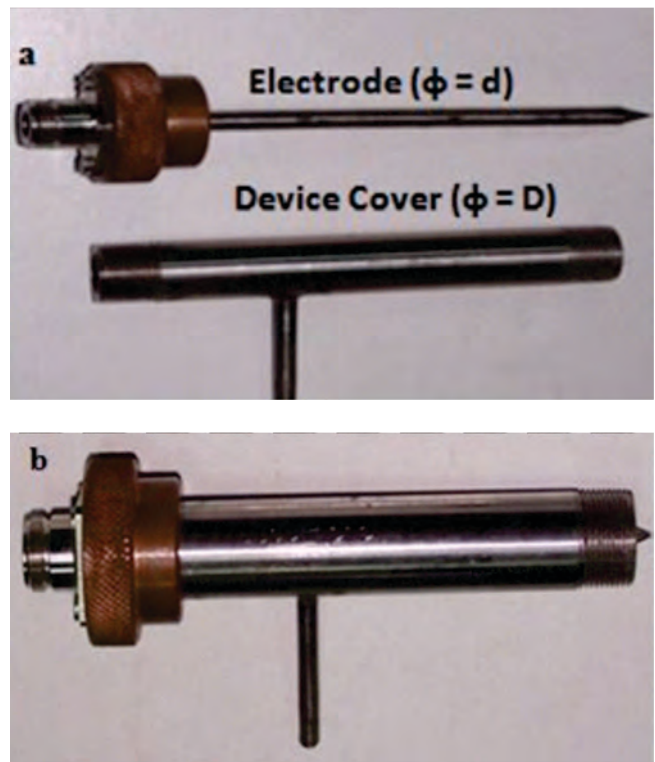
Fig. 1: Photograph of the APPJ device

Fig. 2 shows the schematic and actual set-up where plasma is generated with the APPJ device. A 2.45 GHz magnetron was used to generate microwave which then propagated through a waveguide. The APPJ device was connected to the waveguide through LMR 400 co-axial cable for easy manouvering. Gases were passed through mass flow controllers and gas mixer for plasma generation.

Etching of Tantalum(Ta) Surrogate:

Before using the device inside a glove box, etching of Ta, a known surrogate of Pu was done under two different sets. The
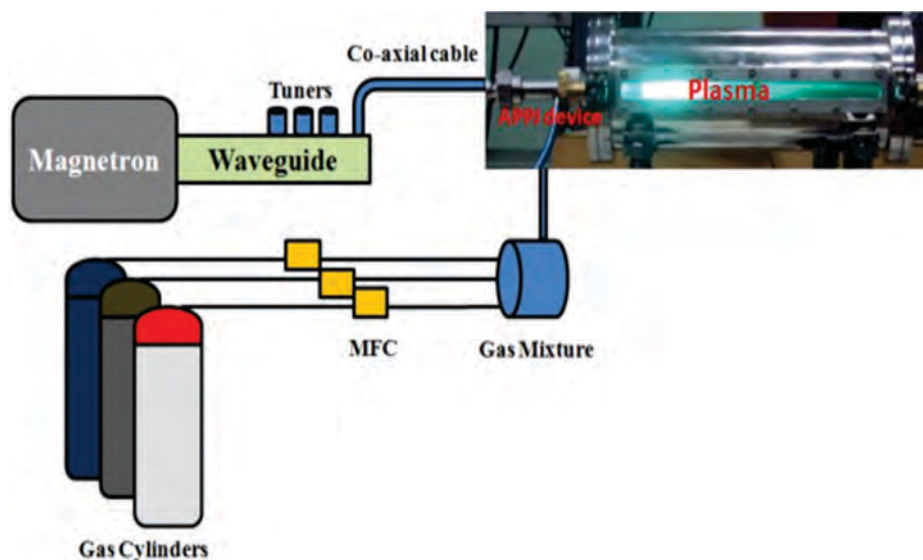
Fig. 2: Schematic and photograph of the experimental set-up

first set had a gas mixture of 3% CF_4 + Ar plasma while O_2 was added in the second set to study its effect in etching. It is seen that O_2 makes plasma etching more aggressive by increasing the etching rate to 4.1 mg/ min [6].

Pu Decontamination inside Glove Box:

The device was next installed inside glove box where synthetic samples of Pu with α activity of 40,000 counts per minute (CPM) were prepared by taking 20 μl $Pu(NO_3)_4$ drops on the centre of SS 304L discs (25 mm diameter). They were then exposed in plasma for 10 minutes. Pu was chosen as the radioactive source since it has one of the highest specific activities among all transuranic elements. A ZnS(Ag) scintillation counter having efficiency of ~ 25% (standardized against [241]Am standard source) was used for measuring α counts before and after each experiment. Decontamination factor (DF) was calculated using equation 2. Higher DF value signifies better removal of waste.

$$DF~(\%) = (Initial~CPM - Final~CPM) /$$
$$Initial~CPM~x~100 \qquad (2)$$

Fig. 3(a) shows that DF increases as much as 15% in presence of O_2 for 200 standard cubic cm (SCCM) flow of CF_4. Fig. 3(b) shows the optimum ratio of CF_4:O_2 observed

experimentally. It is seen that this ratio almost saturates beyond 0.8. Though reduction in Ar flow resulted in improvement of DF value but it was fixed at 6 LPM as plasma jet showed continuous fluctuation below this flow because of increased instability.

Design and Decontamination with Multi-electrode APPJ Device:

Based on the encouraging results obtained with single electrode APPJ device, a multi-electrode model was conceptualized for scaling up decontamination process. Designing a multi-electrode APPJ device was not possible by analytical means for its complex geometry. This device was simulated using time domain and frequency domain solver simulations in CST microwave software. Fig. 4(a) shows the actual multi-electrode device and Fig. 4(b) shows the obtained decontamination result with it.

From the Fig. 4 (b) it is seen that DF increases linearly with decreasing Ar flow rate. The result showed that ~ 95% decontamination can be achieved at 6 LPM Ar flow in 5 mins. When compared with the performance of single electrode device, it was seen that the scaled up multi-electrode model reduced operation time by almost 50%.
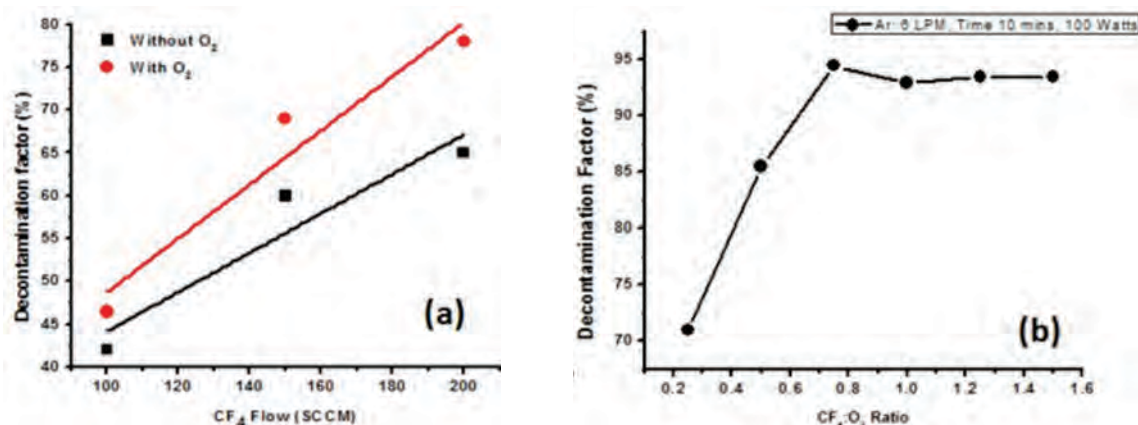
Fig. 2: Schematic and photograph of the experimental set-up
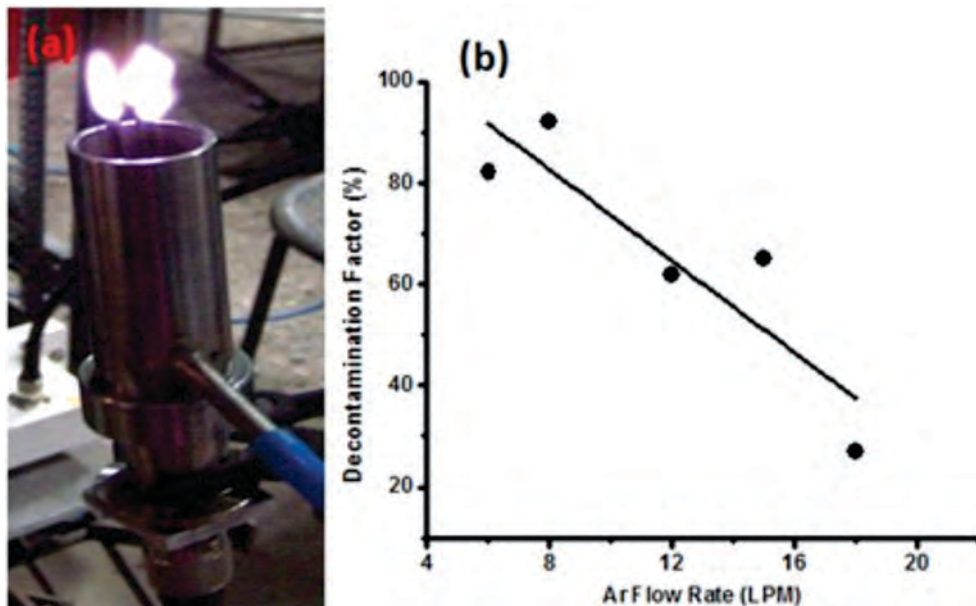
Figure 4: (a) Fabricated multi-electrode APPJ device, (b) variation of decontamination factor with Ar flow

Based on our parametric runs, optimized operational parameters for APPJ devices were chosen to 6 LPM Ar flow along with a mixture of CF_4:O_2 at 1:1 where each of them was kept at 3% to 3.5% of the total gas flow, with input power of 100 Watts. Removal of nuclear waste ~ 95% was observed within 5 mins under optimized conditions with the multi-electrode model. Material balance was also found to be better than 98% in all cases.

To confirm our measured data on alpha activity, a few samples after decontamination were dissolved completely in 8 M HCl and the resulting solution was subjected to radiometry to find the α counts. Number of counts obtained after decontamination experiments matched well with what was obtained in the acidic solution. These tests confirmed that plasma actually removed contamination from the surface.

Plasma probably is the most underused tool in nuclear waste management system & our investigations sufficiently demonstrate the potential. Scaling up was said to be the only difficulty for putting this technology in practice [3, 4] which we have partially solved by showing that this technique can be extended to a multi-electrode device hence allowing larger area to be addressed. However, more research in this direction is needed for further scaling up of this technique for execution of decontamination of larger jobs.

References:

1. Raj K, Prasad K.K, Bansal N.K, "Radioactive waste management practices in India". *Nuclear Engineering and Design,* 236, (2006): 914–30.

2. Windarto H.F, Matsumoto T, Akatsuka H, Suzuki M, "Decontamination Process using CF_4-O_2 Microwave Plasma at Atmospheric Pressure". *J. Nuc. Sci. Tech.* 37, (2000):787-92.

3. Hicks R.F, Herrmann H.W, *Atmospheric-Pressure Plasma Cleaning of Contaminated Surfaces, US dept. of energy, Project Number: 73835 Grant Number: FG07-00ER45857, 2003*

4. Veilleux J.M, Kim Y, "Can Plasma Decontamination Etching of Uranium and Plutonium be Extended to Spent Nuclear Fuel Processing". *Los Alamos National Lab,* 52nd Annual Meeting July 17-21, (2011): 1-4.

5. Jasinski M, Zakrzewski Z, Mizeraczyk J, "New Atmospheric Pressure Microwave Microplasma Source". *Acta Technica CSAV,* 53, (2008): 347-54.

6. Kar R, Bute A, Chand N, Patil D.S, Chandra Romesh, Jagasia P, Dhami P.S, Sinha S, "*Actinide Decontamination by Microwave Atmospheric Pressure Plasma jet: A Systematic Study Supported by Optical Emission Spectroscopy*". Submitted to J. Env. Rad. (Ref: JENVRAD-2018-235)

कृषि अनुप्रयोगों के लिए नगर निगम के सूखे सीवेज आपंक (कीचड़) की विकिरण द्वारा संशोधन

डॉ. ललित वार्ष्णेय एवं डॉ. नरेंद्र कुमार गोयल

विकिरण प्रौद्योगिकी विकास प्रभाग

विकिरण प्रौद्योगिकी:

स्वास्थ्य, उद्योग, कृषि और अनुसंधान जैसे विभिन्न क्षेत्रों में रेडियोसोटोप और विकिरण प्रौद्योगिकी के अनुप्रयोगों में उन्नति ने जीवन की गुणवत्ता में सुधार किया है। विकिरण द्वारा स्वास्थ्य संबंधी उत्पादों का रोगाणुनाशन और खाद्य संरक्षण अभी दो प्रमुख उपयोगितायें हैं जो मानवता के लाभ के लिए महत्वपूर्ण भूमिका निभा रही हैं। भारत में कोबाल्ट-60 स्रोत से गामा विकिरण का उपयोग कर स्वास्थ्य संबंधी उत्पादों का रोगाणुनाशन अच्छे से स्थापित एक औद्योगिक प्रक्रिया है। विकिरण प्रौद्योगिकी का एक और बहुत महत्वपूर्ण अनुप्रयोग सीवेज आपंक का संशोधन है जो न केवल पर्यावरण प्रदूषण की समस्या का समाधान करता है बल्कि कृषि अनुप्रयोगों के लिए बहुत उपयोगी हो सकता है।

सीवेज आपंक संशोधन:

सीवेज घरेलू परिसर से उत्पन्न अपशिष्ट जल है और मुख्य रूप से मानव अपशिष्ट के बने होते हैं। इसमें आमतौर पर 99.9% पानी तथा लगभग 0.1% ठोस से युक्त होता है। सीवेज में ठोस अपशिष्ट का स्वरूप आमतौर पर जैविक होता है और यह सीवेज उपचार संयंत्र से विभाजित हो जाता है जिसके परिणाम स्वरूप सीवेज आपंक सहउत्पाद के रूप में मिलता है। इस सह उत्पाद आपंक को सूर्य विकिरणों में 75-85% तक सुखाया जाता है जिसे सूखा आपंक कहा जाता है। 2-3 मिलियन आबादी वाला शहर एसटीपी पर प्रतिदिन 300 मिलियन लीटर सीवेज से लगभग 100 टन सूखा आपंक पैदा करता है। नगर पालिका के इस सूखे सीवेज आपंक का निष्कासन, विशेष रूप से बड़े महानगरीय शहरों में, शहरी प्राधिकरणों के लिए एक गंभीर समस्या के रूप में उभर रहा है क्योंकि आपंक में संभावित संक्रामक सूक्ष्मजीव बहुतायत में होते हैं जो सार्वजनिक स्वास्थ्य के लिए गंभीर खतरा हो सकता है।

आपंक निष्कासन के वर्तमान तरीकों की अपनी सीमाएं हैं। उदाहरण के लिए, समुद्र में निपटान साइट विशिष्ट है, जलाए जाने की प्रक्रिया एक अत्यंत ऊर्जा गहन प्रक्रिया है और भूमि भरने की प्रक्रिया में शहरी इलाकों में दुर्लभ भूमिकी

उपलब्धता के कारण दूर की जगह आपंक का परिवहन शामिल है। दूसरी ओर आपंक दीर्घ एवं सूक्ष्म पोषक तत्वों जैसे नाइट्रोजन, फ़ासफ़ोरस, पोटैशियम तथा ज़िंक, आयरन, ताम्र आदि का एक महत्वपूर्ण स्रोत है। खेती समुदाय के साथ-साथ सीवेज उपचार संयंत्र (एसटीपी) ऑपरेटरों में आपंक के कृषि में अनुप्रयोग हेतु रुचि बढ़ी है।

सूखी सीवेज आपंक (सूखे आपंक) को फसलों को पोषक तत्वों की आपूर्ति, मिट्टी की भौतिक गुणधर्मों में सुधार और मिट्टी के जैविक पदार्थों को बढ़ाने के लिए लाभकारी रूप से उपयोग किया जा सकता है। इसके परिणामस्वरूप फसल उत्पादकता में बढ़ोत्तरी और साथ ही मिट्टी की उर्वरता की बहाली भी हो सकती है। यह तरीका सीवेज उपचार संयंत्र (एसटीपी) ऑपरेटरों के लिए कचरे से बहुमूल्यता

सहउत्पाद प्राप्त करने का रास्ता प्रदान कर सकता है जिसका निष्कासन अन्यथा पर्यावरण संबंधी चिंता का विषय और राष्ट्र का आर्थिक नुकसान है। इसलिए, कृषि अनुप्रयोगों के लिए सीवेज आपंक की पुनरावृत्ति एक महत्वपूर्ण केन्द्र के रूप में उभर सकता है, बशर्ते इसे ऐसे तरीके से किया जाये जो मानव और पशु स्वास्थ्य के साथ-साथ बड़े पैमाने पर पर्यावरण की सुरक्षा करता हो।

उपर्युक्त सूखे आपंक के उपचार में विकिरण प्रौद्योगिकी महत्वपूर्ण भूमिका निभा सकती है और इसे कृषि अनुप्रयोगों के लिए मूल्यवर्धित उत्पाद खाद में परिवर्तित किया जा सकता है। सीवेज आपंक के विकिरणन का योजनाबद्ध चित्र-1 में दर्शया गया है। उच्च ऊर्जा विकिरण में एक सरल, कुशल और विश्वसनीय तरीके से सीवेज आपंक में मौजूद सूक्ष्म जीवों को निष्क्रिय करने की अनूठी क्षमता है। कोबाल्ट-60 जैसे विकिरण स्रोत द्वारा उत्सर्जित आयनिक विकिरण, कोशिकाओं में मौजूद डीएनए, प्रोटीन और पानी जैसे महत्वपूर्ण अणुओं के साथ अंतःक्रिया करते हैं जिसके परिणामस्वरूप रोगजनकों की निष्क्रियता होती है। इस गुण के कारण, विकिरण प्रौद्योगिकी सार्वजनिक स्वास्थ्य के क्षेत्र में काफी उपयोगी है। एक मानक सीवेज उपचार संयंत्र का
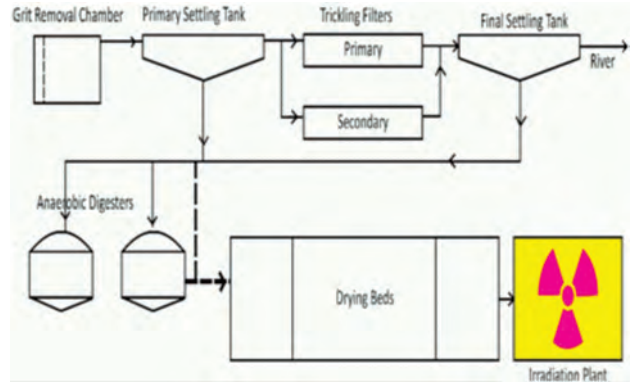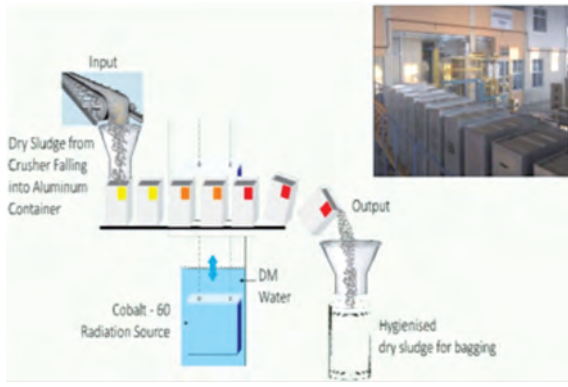
चित्र-1: योजनाबद्ध तरीके से सीवेज आपंक का संशोधन एवं मानक एसटीपी का स्वरुप

अंतिम उत्पाद सूखी मिट्टी होता है जिसमें लगभग 75-80% ठोस और 20-25% पानी होता है।

कीचड़ विकिरणन संयंत्र (चित्र: 2) को या तो एसटीपी के साथ एकीकृत किया जा सकता है या किसी अन्य स्थान पर स्थित हो सकता है जो क्षेत्र में मौजूद अन्य एसटीपी के लिए केंद्र बिंदु के रूप में कार्य कर सके। अपने आप में इस तरह की पहली सुविधा अहमदाबाद में, अहमदाबाद नगर निगम के साथ शुरू हो रही है, जोकि अप्रैल, 2018 तक शुरू होने की उम्मीद है। यह सुविधा 30 करोड़ की लागत से लगभग 4500 मीटर वर्ग क्षेत्र में आ रही है जो शहरी कीचड़ को रू.1000/- प्रति टन के हिसाब से संशोधित कर सकता है। विकिरण संशोधित आपंक में रोगनाशक कीटाणुओं के मरने के कारण उपयोगी जीवाणुओं जैसे राइज़ोबियम, एज़ोटोबैक्टर इत्यादि को पनपने का एक आदर्श माध्यम है जिनका छिड़काव संशोधन के बाद किया जाता है। इस प्रकार इसे मूल्य युक्त खाद में परिवर्तित करते हैं जिससे इसकी वाणिज्यिक उपयोगिता बढ़ जाती है।

विकिरण संशोधित आपंक में निम्नलिखित निर्दिष्ट सीमाओं से अधिक नहीं होना चाहिए:

1. प्रदूषक जैसे आर्सेनिक, कैडमियम, क्रोमियम, तांबा, सीसा, पारा, निकल, सेलेनियम और जस्ता की उपस्थिति। किन्तु घरेलू सीवेज में इन धातुओं की सान्द्रता अधिक नहीं होती है। शहरी विकास मंत्रालय (एम. ओ. यू. डी., भारत) और संयुक्त राज्य अमेरिका के पर्यावरण संरक्षण एजेंसी (यूएसई.पी.ए.,40 सीएफआर 503) ने भी समान परिसीमाएं बताई हैं।

2. रोग जनकों की मौजूदगी (जैसे बैक्टीरिया, वायरस, परजीवी)

3. सीवेज आपंक के प्रतिवेक्टरों जैसे कृन्तक, मक्खी, मच्छर, पक्षी का आकर्षण जो अन्य जगहों और मानवों से रोग ज़नकों को स्थानांतरित कर सकते हैं। एसटीपी प्रक्रिया इस कारक को कम कर देता है।

सूखे कीचड़ की विकिरण स्वच्छता प्रक्रिया के फायदे:

1. सरल, प्रभावी, किफायती, पुनरुत्पादनीय तथा आरोह्य प्रक्रिया।

2. मौजूदा पारंपरिक सीवेज उपचार सुविधा प्रक्रिया के साथ एकीकृत करने में आसान है और इस क्षेत्र में अन्य एसटीपी के लिए एक केंद्र बिंदु के रूप में भी इस्तेमाल किया जा सकता है।

3. डिज़ाइन, कमीशन और संचालन पूर्ण रूप से स्वदेशी तकनीक है तथा हस्तचालन से बचने के लिए पूरी तरह से स्वचालित बनाया गया है।

4. यह प्रक्रिया विकिरण चिकित्सा उत्पाद के जीवाणुनाशन प्रक्रिया की आधार पर विकसित की गई है जो पूरी दुनिया और भारत में पूरी तरह से स्थापित है।

5. संशोधित आपंक संभवतः एक उपयोगी जैविक खाद के साथ आवश्यक मानकों के जैव-उर्वरक उत्पादन का एक अच्छा विकल्प है।
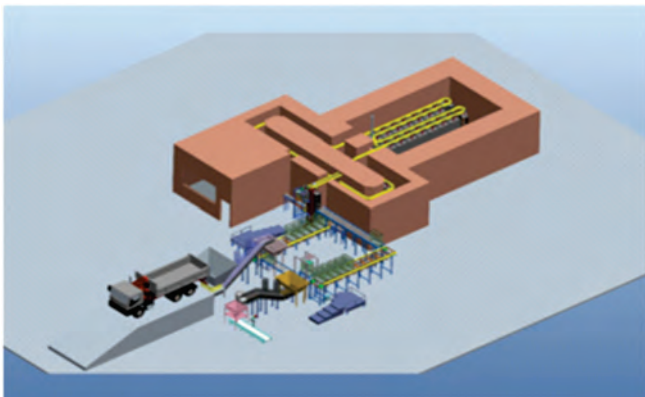
चित्र-2: विकिरणन संयंत्र के साथ आगामी संयंत्र इमारत का दृश्य

Ab initio Calculations to Understand Ionic Conduction in Lithium Ion Battery Materials

Mayanak K. Gupta[1], Baltej Singh[1,2], Prabhatasree Goel[1], Ranjan Mittal[1,2] and Samrath L. Chaplot[1,2]
Solid State Physics Division[1]
Homi Bhabha National Institute[2]

We have performed first principles simulations on Lithium ion conductors, namely, Li_2O, $LiMPO_4$(M=Fe, Mn) and $LiAlSiO_4$. We are able to identify the specific vibrational mode of lithium ions that become soft at high temperature and which may lead to onset of the superionic behaviour in Li_2O. The mode belongs to the transverse-acoustic phonon branch at the Brillouin-zone boundary and involves large displacement of the lithium ions in the [100] direction. In another battery material, $LiMPO_4$ (M=Fe, Mn), the lattice dynamics calculations reveal instability of some phonon modes when the unit cell volume is increased to that corresponding to elevated temperature, which may result in the onset of diffusion of Li in these compounds. The ab initio molecular dynamics simulations for $LiAlSiO_4$ reveal the nature of the one-dimensional superionic conduction which involves correlated jump diffusion of lithium ions.

Keywords: Ab initio simulation, Phonon, Lattice dynamics, Molecular dynamics

Introduction

Fast ion conductors are one of the functional materials which possess high values of ionic conductivity at relatively modest temperatures. Such compounds find extensive technological applications in solid state batteries, gas sensors and fuel cells. The search for better solid electrolytes (i.e. higher ionic conductivities, higher power densities, low cost, environmentally friendly, etc.) is a particularly active area of research. Discovery and exploitation of new high-performance materials requires a greater fundamental understanding of their properties on the atomic scales, leading to major advances in rechargeable batteries for portable electronics, electric vehicles and large-scale grid storage. Also, global warming and diminishing fossil fuel reserves accelerate the search for efficient energy alternatives. The performance of energy storage devices depends crucially on the properties of their component materials. An excellent example of innovative materials science is the discovery of the rechargeable lithium battery.

Materials research based on computational methods now plays a vital role in characterizing and predicting the structures and properties of complex materials on the atomic

scale. The simulations are able to predict the material properties at extreme conditions as well as supplement the experimental studies. Here we review our work based on first principles simulations to understand the diffusion mechanism of Li ion in superionic conductor Li_2O [1,2], $LiMPO_4$ (M=Fe, Mn)[3] and $LiAlSiO_4$[4-6]. The comparison between the calculated and experimental neutron inelastic spectra for these compounds is shown in Fig 1. The general characteristics of the experimental features are well reproduced by the lattice dynamics calculations. The motivation and significant results from our studies on various compounds are discussed below.

Soft-phonon mode in Li_2O

The compound Li_2O belongs to the class of superionic conductors, which exhibit high ionic conductivity above 1200 K. In this case, Li ions are the diffusing species, while oxygen ions constitute the rigid framework. The material finds large applications mostly due to its high melting point, relatively low volatility and high Li atom density. At ambient conditions, Li_2O occurs in the anti-fluorite structure [7-9]. Oxygen ions are arranged in a face centered cubic (FCC) sub lattice with lithium ions occupying the tetrahedral sites.
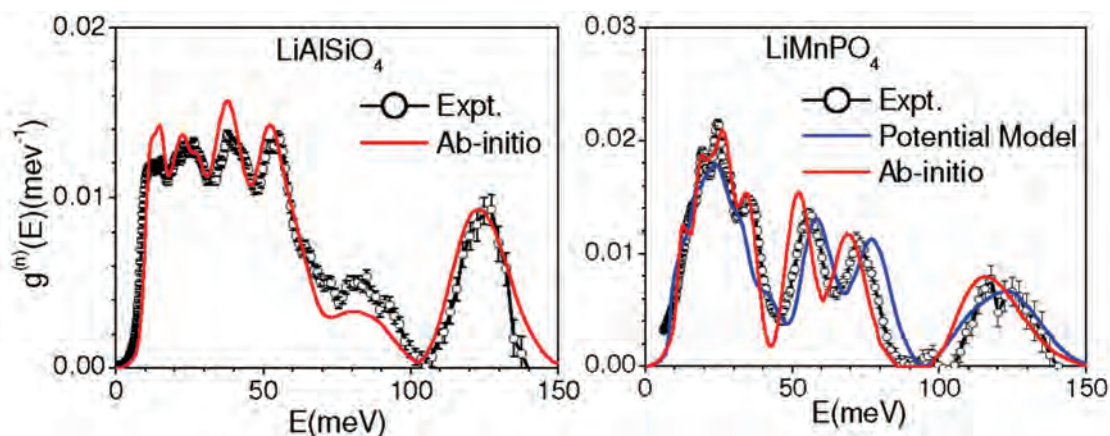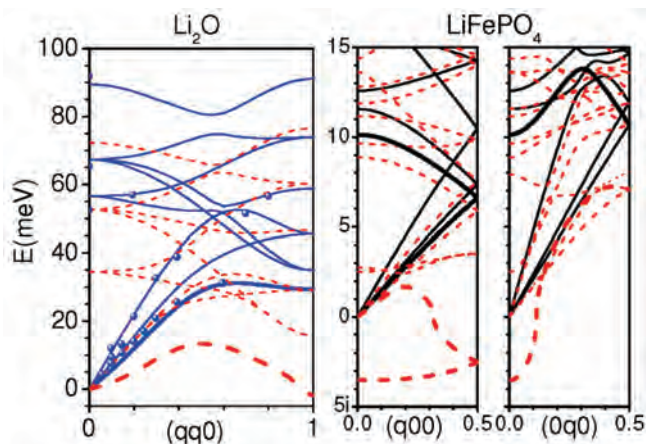

Fig. 1: The comparison of the calculated (at 0 K) and experimental (at 300 K)neutron inelastic scattering spectra for $LiAlSiO_{4[5]}$and $LiMnPO_4$[3].

The calculated phonon dispersion [1] relation (Fig. 2) at relaxed lattice parameter a = 4.57 Å (at 0 K) are in good agreement with the reported experimental data. The compound exhibits superionic transition in the vicinity of 1200 K. Hence, we have performed phonon calculations at various unit cell parameters corresponding to high temperatures. As expected, the phonon frequencies along all three directions are found to soften with the increase of volume[1]. The softening is found to be small for all the modes except for the lowest transverse acoustic (TA) branch along [110] direction at zone boundary.

The eigen-vector of unstable transverse acoustic mode of Li_2O has been plotted (Fig. 3), which shows displacements of lithium atoms along [001] direction while the oxygen atoms are at rest. It is possible that the softening of these modes might be the precursor to the process of diffusion. At the superionic transition, some of the lithium atoms might just have sufficient energy to move from their ideal positions and start diffusing. Increasing the temperature could lead to
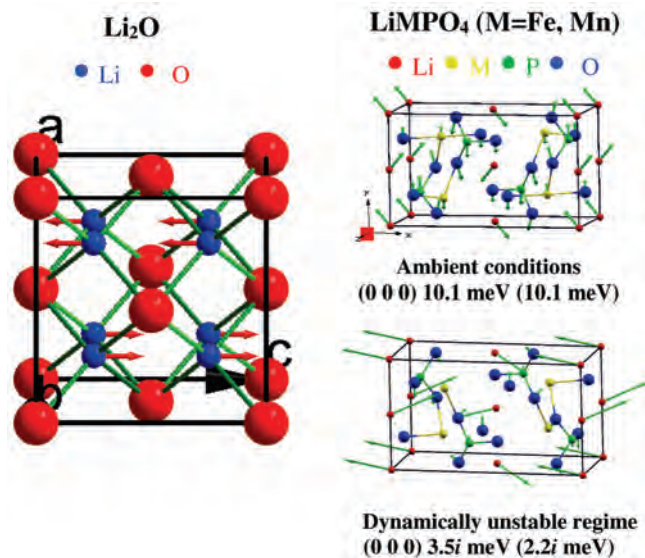

Fig. 3: (Left) Motion of individual atoms for the transverse acoustic mode at zone boundary at (110)[1]. (Right)Motion of individual atoms for zone centre mode at unit cell volumes corresponding to room temperature and dynamically unstable regime (1500 K and 900 K in $LiFePO_4$ and $LiMnPO_4$ respectively)[3]. The numbers after the mode assignments give the phonon energies of mode in Fe (Mn) compound. The letter 'i' after the phonon energy indicates that mode is unstable.

Fig. 2: (Left)The calculated phonon dispersion relation for Li_2O[1].The full and dashed lines correspond to calculations performed at volume corresponding to room temperature and superionic regime (1200 K) respectively. The solid symbols correspond to reported experimental–[20] data at room temperature. (Right) The low-energy part of the phonon dispersion relation calculated for $LiFePO_4$[3]. The full and dashed lines refer to the calculations corresponding to the volume at room temperature and 1500 K for $LiFePO_4$. The thick lines show the phonon branches undergoing large softening.

migration of lithium ions along [001] direction.

Soft-phonon modes in $LiMPO_4$ (M=Fe, Mn)

Another important battery material $LiMPO_4$(M= Fe, Mn), used as cathode material, crystallize in olivine type orthorhombic Pnma[10] space group analogous to mineral Triphylite structure. The structure comprises of discrete PO_4 tetrahedra and highly distorted oxygen octahedra about lithium and transition metal ion, M. The PO_4 tetrahedra are irregular, with two significantly different sets of O-O distances. We have performed the lattice dynamics and molecular simulations along with inelastic neutron scattering measurements to understand the diffusion of Li ions.

The calculated phonon frequencies of $LiMPO_4$ (M=Fe, Mn)

along all the high symmetry directions (Fig. 2) are found to soften with increase of volume. However, the softening is found to be very large for one of the phonon branches along [100] direction. We find that in both the compounds the zone centre optic mode softens first, followed in quick succession by the zone-boundary mode along [100] direction with increasing volume.

For qualitative understanding of the atomic displacement in $LiMnPO_4$ compounds, we have plotted eigen-vectors of unstable modes (Fig. 3). In case of the zone-centremode at ambient volume the displacements of the Li atoms are maximum, while the amplitudes of other atoms are less but not negligible. The displacement of the lithium ions is only in the x-y plane. In the dynamically unstable regime, the amplitude of Li atoms has increased significantly. The Fe atoms are at rest, while the amplitude of P atoms decreased slightly and O atoms do not show any change. The component of displacement of Li atoms is non-zero along all the three directions but with the highest component along the x-direction.

We find that $LiFePO_4$ shows softening (Fig. 2) at a higher volume in comparison with the Mn counterpart. The percentage change in volume for initiation of phonon instability in $LiMnPO_4$ is much lesser as compared to $LiFePO_4$.

The main interest in these compounds stems from their use as battery materials. Lithium intercalation and subsequent delithiation are the main processes by which energy is transferred during its use as battery material. We have tried to unveil the role of phonons in the initiation of lithium movement crucial for the use of these materials as battery material. Our analysis shows that at ambient temperature, the

likely motion of lithium is in the x-y plane. If conducive conditions prevail, lithium might move in this plane.

Ab initio molecular dynamics of LiAlSiO$_4$

LiAlSiO$_4$ (β- eucryptite) is a very important one- dimensional superionic conductor. It possesses superionic conductivity along with anisotropic negative thermal expansion (NTE) behaviour[5,6,11,12]. LiAlSiO$_4$ has a hexagonal structure[13] (space group P6$_2$22) that expands in the ab-plane and contracts along the c- axis upon heating. It shows an overall very low volume thermal expansion [14,15] and has good mechanical stability. These properties make it a potential electrolyte for Li ion batteries[16]. Lithium is decorated in one-dimensional channels parallel to the hexagonal c-axis. The room temperature structure has two types of channels[17], namely, '*S*' type and '*A*' type. In '*S*' type channel *Li* atoms are coplanar with the *Si* atoms while in '*A*' type channel *Li* atoms are coplanar with the *Al* atoms. There are three secondary (*S*) and one primary (*A*) channel in a single unit cell of the room temperature structure[17]. On heating at around 700 K, a phase transition occurs by disordering of Li among all the available sites along the c-axis. The high-temperature phase exhibits a one-dimensional superionic Li conduction.

We have performed ab initio molecular dynamical simulations to understand the mechanism of the high-temperature (HT) phase transition and superionic conduction in the HT phase. The mean square displacements of various atoms (Li, O, Al & Si) are calculated (Fig. 4a) from the time evolution of the trajectory of these atoms at room temperature (300K). The temperature, pressure and energies are well converged in these calculations. The calculated mean square amplitudes (Fig. 4a) show that the Li being lightest element has the highest but Al and Si being heavier has lower mean square amplitudes.

As simulation temperature is increased to 600 K, we see (Fig 4b) that although Al, Si, and O atoms have very small and almost constant values of mean square displacements, Li atom shows a sudden increase after 4 pico seconds. We analyzed the anisotropic mean square displacements (MSD) (Fig. 4c) for Li atoms and found that the MSDs show an anomalous value only along the hexagonal c-axis while it is negligible in the *ab*-plane. This implies that Li atoms move along the hexagonal c-axis with a jump like behaviour. When the trajectories of all individual atoms (Fig. 4d) are analyzed, we found that groups of three Li atoms are moving altogether. A group of three Li atoms belong to the same channel. The very first channel movement (Fig. 4d) occurs around a simulation time of 4 ps. This is found to be the 'A' type channel. All the Li atoms in this 'A' type channel are found to have squared-displacement of ~3.6 Å^2 which corresponds to a displacement of ~1.9 Å. This displacement is equal to c/6. This indicates that the 'A' type channel is transformed to the 'S' type channel. Afterwards, the Li atoms (three atoms together) in other channels also start moving along c-axis with displacement amplitude of about c/6 and c/3 etc. Hence Li atoms have a possibility to be present in all the available sites along the channels at 600K. All the

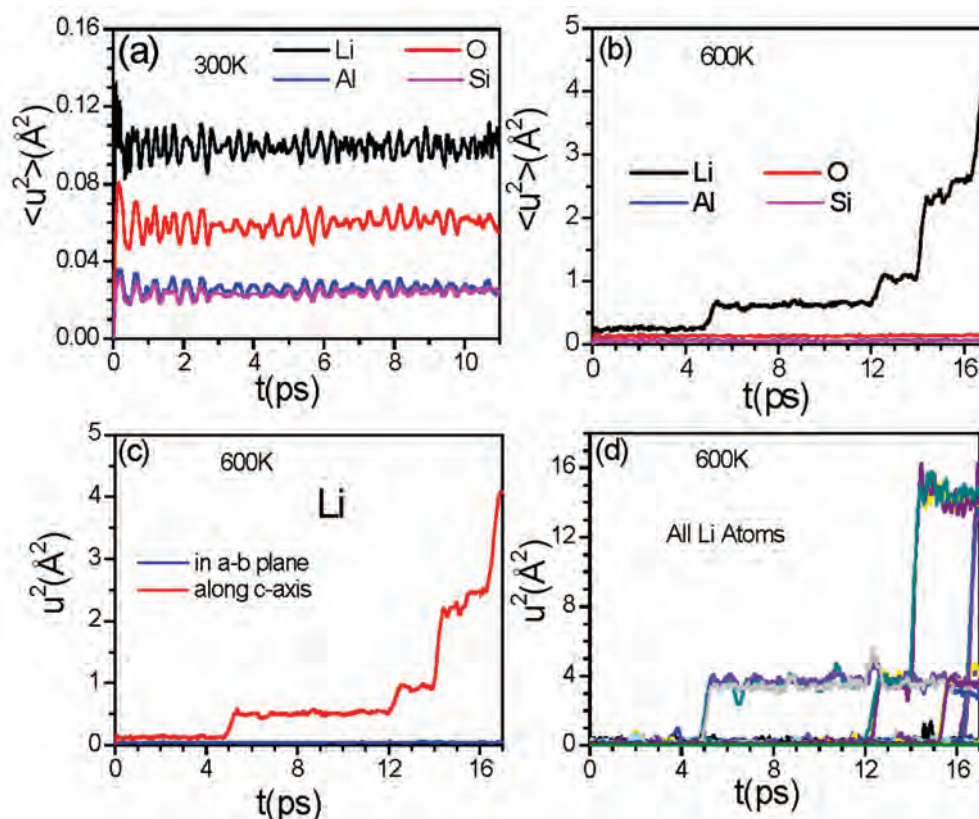**FIG 4** The calculated mean-squared displacements (<u^2>) of various atoms of RT- phase of β-eucryptite as a function of time (a) at 300K and (b) 600K. (c) Anisotropic mean-squared displacement (<u^2>) of Li averaged over all the Li atoms in the supercell and (d) u^2 of each individual Li atoms along c-axis at 600K as a function of time[4].

channels become equivalent with a distribution of Li atoms at all the available sites. This gives rise to the high- temperature phase transition in β-eucryptite [13]. This transition was experimentally reported [13,18] at 698-758 K. In the high temperature phase, all channels become equivalent and the hence the new symmetry reduces the 'a' (or 'b') lattice parameter to half of their original values. Experimentally[18] the high temperature structure of β-eucryptite is also known to have Li atoms positional disordering along the hexagonal c-axis.

The simulations performed at 800 K in the HT phase indicate increase in Li channel movements. At 800 K (Fig. 5a & Fig. 6a), the compound is already in high temperature structure, so all the Li containing channels are equivalent. The channel movement begins at smaller simulation time in comparison to

that for 600 K, and some channels start moving coherently at the same time. The increasing squared displacements (u^2) of Li atoms in these channels signify the diffusion in Li channels along the hexagonal c-axis. When temperature is raised to 1000 K (Fig. 5b & Fig. 6b), more numbers of channels are seen to be diffusing at even smaller simulation times. During the diffusion, there is correlation between the Li atoms in each channel which can be seen at 1000K (Fig. 5b & Fig. 6b). The diffusion of Li channels in this compound is found to be one-dimensional jump-like rather than continuous diffusion. At sufficiently high temperature of 1200 K (Fig. 6c), some of the Li atoms also started diffusing in the ab-plane; hence at high temperatures the intra-channel correlation of Li atoms decreases.

We have calculated the average diffusion coefficient for all the
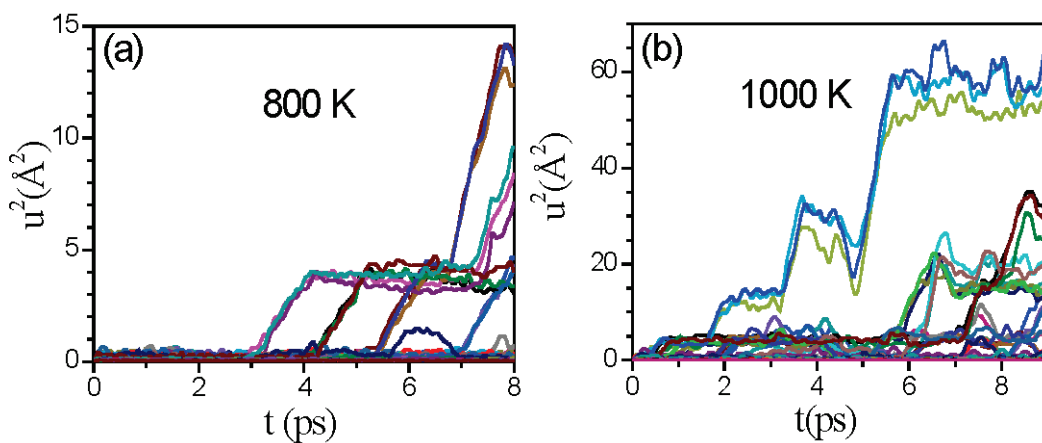
Fig. 5: The calculated u^2 of each individual Li atoms of HT- phase of β-eucryptite as a function of time along c-axis at (a) 800K (in 331 supercell), (b) 1000K (in 331 supercell)[4]

(a) T=800K, HT Phase Supercell (3×3×1)

(b) T=1000K, HT Phase Supercell (3×3×1)
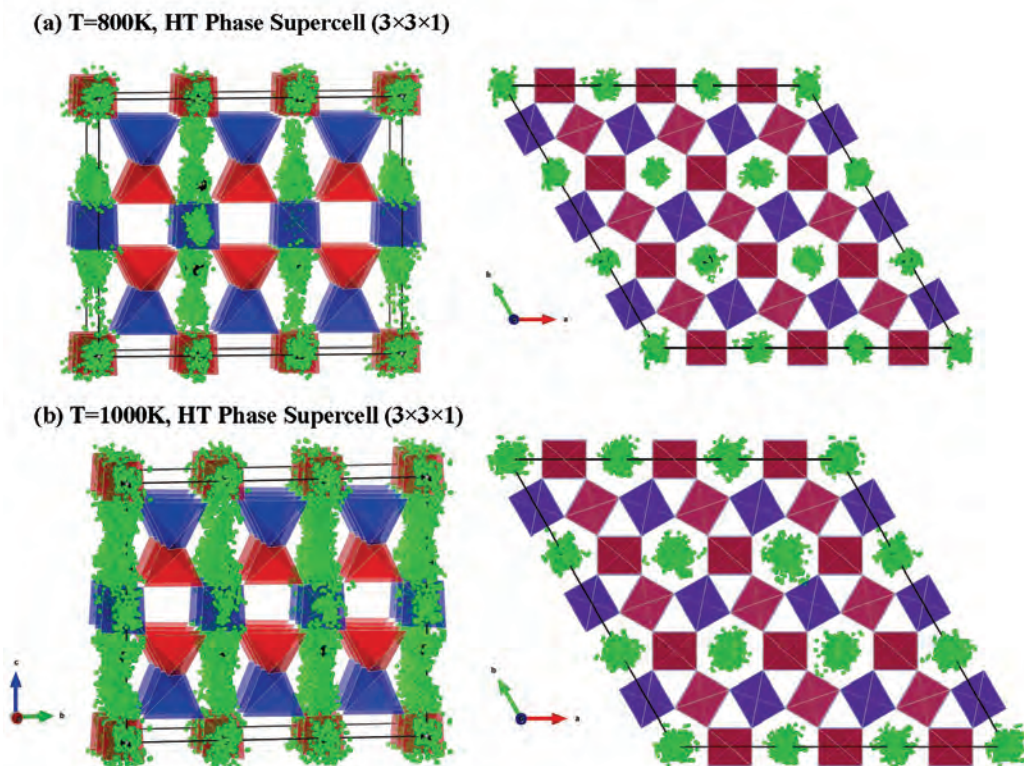
Fig. 6: Trajectory of Li atoms in channels of β-eucryptite (HT-Phase) at (a) 800K and (b) 1000K. Key: AlO$_4$-Blue, SiO$_4$-Red, Initial Position of Li- Black, Time Evolution of Li- Green balls[4]
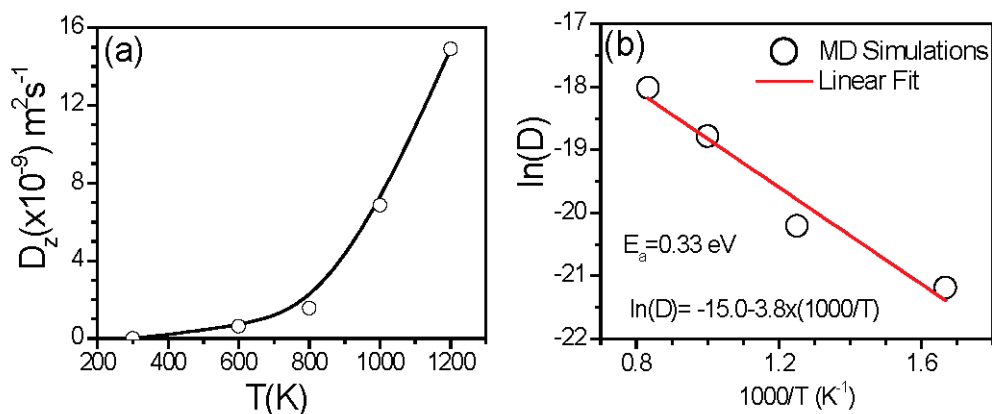
Fig. 7: The calculated (a) one-dimensional diffusion coefficient as a function of temperature and (b) Arrhenius plot of diffusion coefficient and temperature to obtain activation energy for Li diffusion[4].

Li atoms in the supercell. The calculated diffusion coefficient (Fig. 7a) shows a sharp increase in magnitude around 600K. The calculated value of diffusion coefficient has magnitude ($\approx 10^{-9}$ $m^2 s^{-1}$) comparable to that of atoms in liquids. So, the high temperature structure of β-eucryptite possesses a superionic Li conduction which is one dimensional in nature. The activation energy for Li jump diffusion can be obtained from the Arrhenius plot of diffusion coefficient. The calculated activation energy (Fig 7b) for diffusion of Li atoms is 0.33 eV which agrees with those calculated [6] from the nudged elastic band method (0.3-0.4 eV) and with the experimental [19] values of 0.6-0.8 eV.

Conclusions

First principles calculations of Li_2O, $LiMPO_4$ (M=Fe, Mn) and $LiAlSiO_4$ have been successfully used to understand the atomic vibrations and their role in ionic diffusion in these compounds. The calculated phonon dispersion relation in Li_2O and $LiMPO_4$ (M=Fe, Mn) as a function of volume suggests a significant phonon instability which may be related to initiating the diffusion of lithium ions. For $LiAlSiO_4$, ab-initio molecular dynamical simulations are used to understand the mechanism of the high-temperature phase transition and superionic conduction. The simulations for $LiAlSiO_4$ reveal one-dimensional jump-like diffusion of lithium ions in the compound.

References

1. M. K. Gupta, P. Goel, R. Mittal, N. Choudhury, and S. L. Chaplot, Physical Review B 85, 184304 (2012).

2. P. Goel, N. Choudhury, and S. L. Chaplot, Physical Review B 70, 174307 (2004).

3. P. Goel, M. K. Gupta, R. Mittal, S. Rols, S. J. Patwe, S. N. Achary, A. K. Tyagi, and S. L. Chaplot, Journal of Materials Chemistry A 2, 14729 (2014).

4. B. Singh, M. K. Gupta, R. Mittal, and S. L. Chaplot, Journal of Materials Chemistry A 6, 5052 (2018).

5. B. Singh, M. K. Gupta, R. Mittal, M. Zbiri, S. Rols, S. J. Patwe, S. N. Achary, H. Schober, A. K. Tyagi, and S. L. Chaplot, Journal of Applied Physics 121, 085106 (2017).

6. B. Singh, M. K. Gupta, R. Mittal, M. Zbiri, S. Rols, S. J. Patwe, S. N. Achary, H. Schober, A. K. Tyagi, and S. L. Chaplot, Physical Chemistry Chemical Physics 19, 15512 (2017).

7. R. Shah, A. De Vita, V. Heine, and M. C. Payne, Physical Review B 53, 8257 (1996).

8. L. V. Azároff, Journal of Applied Physics 32, 1658 (1961).

9. Y. Duan and D. C. Sorescu, Physical Review B 79, 014301 (2009).

10. S. Geller and J. L. Durand, Acta Crystallographica 13, 325 (1960).

11. U. V. Alpen, E. Schönherr, H. Schulz, and G. H. Talat, Electrochimica Acta 22, 805 (1977).

12. R. Mittal, M. K. Gupta, and S. L. Chaplot, Progress in Materials Science 92, 360 (2018).

13. H. Guth and G. Heger, North-Holland, (1979).

14. L. Xia, G. W. Wen, C. L. Qin, X. Y. Wang, and L. Song, Materials & Design 32, 2526 (2011).

15. H. Xu, P. J. Heaney, D. M. Yates, R. B. Von Dreele, and M. A. Bourke, Journal of Materials Research 14, 3138 (1999).

16. R. T. Johnson, B. Morosin, M. L. Knotek, and R. M. Biefeld, Physics Letters A 54, 403 (1975).

17. W. W. Pillars and D. R. Peacor, American Mineralogist 58, 681 (1973).

18. A. Sartbaeva, S. A. Redfern, and W. T. Lee, Journal of Physics: Condensed Matter 16, 5267 (2004).

19. H. Böhm, physica status solidi (a) 30, 531 (1975).

20. S. Hull, T. W. D. Farley, W. Hayes, and M. T. Hutchings,

Article

Development of Hull Rinser for Head End Process of Spent Fuel Reprocessing

Shaji Karunakaran, G. Sugilal and K. Agarwal
Technology Development Division,
Nuclear Recycle Group

Rinsing of hull before disposal is presently carried out as manual remote operation. Automation of head end operation of future reprocessing plant will require automated hull rinsing equipment complementing the chopping and dissolution processes. Hull rinsing technology based on vibrating helical tray carrying hulls in rinsing solution has been evolved going through the stages of conceptual design, engineering detailing, prototype manufacturing and trials with simulated hulls. The feasibility of concept, amenability for remote operation and maintenance as well as reliability ensures the availability of technology for future high throughput automated plants.

Introduction

Automation in head end process of reprocessing is one of the areas of interest for Nuclear Recycle Group and work has been underway for development of equipment to achieve the same. This will also aid in the design of large throughput plant based on continuous process as against the present batch process. The head end process (Fig.1)consists of following operations: spent fuel chopping, dissolution, feed clarification & hull disposal. Development of Spent Fuel Chopper (SFC) [1] based on gang chopping and its deployment in present operating plant has yielded excellent results. On similar lines development of Continuous Rotary Dissolver (CRD)[2] and Centrifugal Clarifier [3] are under progress. The article presented here elaborates the effort under taken to conceptualize, design, fabricate and testing of hull rinsing equipment which forms an important part of hull disposal process.

Hull Rinsing- Present Methodology

Dissolution in present operating plants is achieved in a dissolver which is a vertical cylindrical vessel housing a perforated basket. The basket receives one batch of chopped fuel pieces from the spent fuel chopper, which is treated with nitric acid for dissolution of heavy metal. The basket retains the hulls while the solution is transferred from the dissolver

for subsequent process. In order to rinse the hulls before its disposal, the dissolver is fed with 2-3 M Acid, which is agitated with air sparging. As a second stage operation, this process is repeated with water. The dissolver basket is then removed from dissolver and placed within the hull tilting equipment for transfer of hulls into a hull drum in a manual remote operation.

Automated Hull Rinsing

Future reprocessing plants with automated head end process will require automated hull rinsing equipment. The equipment shall receive the hulls from continuous dissolver without disturbing the negative atmosphere, rinse it to remove any loose particulate sticking and discharge it into drum which can be sent for disposal. This will eliminate all the manual remote handling operation practiced in present operating plant.

A hull rinsing equipment was conceptualized, designed, fabricated and tested to meet the above requirement, details of which are presented in this article.

Design Concept

The design is based on concept of movement of hulls upward along a helical path in a rinsing medium. The motive force for this upward movement is directional vibration achieved by means of vibratory motor. The system consists of helical trays made of structural material, a pair of vibratory motors mounted in diametrically opposite to central base cylinder, parallel but with 90° phase difference. During operation one of the motor rotates in clockwise while other in anti-clockwise direction. This creates a vibration which assists the movement of vibrating hulls in the desired direction. As the hulls are transferred due to vibration while immersed in rinsing liquid, the dual purpose of transfer of hulls as well as rinsing could be achieved. However, the presence of liquid has tendency to damp the vibration and hence selection of
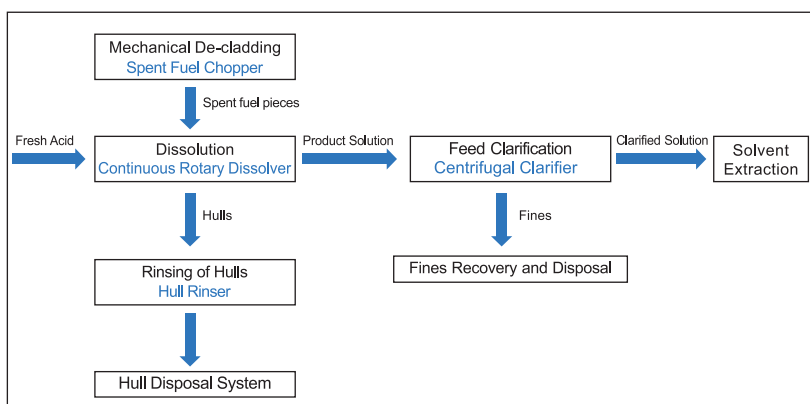
Fig. 1: Head End Process

vibratory motor plays an important role in the functioning of the hull rinser. An important factor of design is also the amenability for meeting the remote operation and maintenance requirement of hot cell application.

Design Features

The basic objective of hull rinser, as mentioned above, is to receive the hull discharged from the dissolver, rinse, and transfer the hulls to a hull drum for disposal (Fig. 2). As equipment in series with Continuous Rotary Dissolver, which discharges the hull, it is essential that the negative atmosphere of the dissolver is not breached during the hull discharge process. Further, it is vital that all components which demand maintenance shall be amenable to remote handling.

Considering these aspects, the hull rinser is designed to have a rectangular tank filled with water, a structural support frame encasing the tank supporting the vibrator and the helical tray assembly (Fig. 3). The discharge chute of the CRD (which is the feed chute for hull rinser) will be immersed in the liquid, acting as water seal to maintain the requisite negative pressure during operation. The design of the hull rinser also facilitates remote removability of the drive assembly for maintenance purpose.

The inlet chute of hull rinser has been designed to receive one batch of hulls, which is fed to bottommost flight of helical tray (Fig. 3). The directional vibration of assembly arising due to operation of mounted vibratory motors drives the hulls upwards along the helical flights. The system is designed to have 75 % of total flights immersed inside the liquid while remaining flights above the liquid level. The vibrating hulls gets rinsed in the liquid as it moves up along the spiral path. As the hulls emerges out of the liquid it is allowed to dry with provision for hot air curtain provided through spray nozzle.

Fig. 2: Hull Rinser in Series with SFC and CRD.

Fig. 3: Hull Rinser

Prototype Development

An engineering scale prototype of Hull Rinser was manufactured (Fig. 4). All the structural material of spiral elevator i.e the spiral flights, base cylinder, motor mounting frame, fasteners has been made of SS 304 L to withstand the acidic environment. The fabrication of the all stainless steel structural assemblies were carried out using TIG welding process. The individual flights were formed with adequate skirting (to prevent fall of shells) and welded to each other around the central cylinder to form helical tray assembly (Fig. 5). The helical tray assembly are mounted with springs which absorbs and transfers the load on structural support. The material of construction for spring is hard chrome plated spring steel. Standard vibratory motor(Fig.6) has been used for the application. The selection of vibratory motor has been

based on the consideration of transfer of the shells in liquid medium which could damp the vibration significantly. The support frame as well as the tank has been made of structural grade carbon steel, this being an experimental prototype.

After completion of manufacturing, the hull rinser was installed at Engineering Hall of CDCFT Facility in WIP, Trombay. Shells made of Aluminum were used to simulate the size and weight of Zircaloy Hulls of PHWR fuel . Rinsing trials (Fig. 7) of shells were carried out after mixing it with powder slurry to check the intended performance of the equipment. Fig. 8. and Fig. 9. represent the pictures of the simulated hull prior to rinsing and after rinsing respectively. In order to quantify the rinsing performance, the trials were carried out with 100 shells which were weighed initially. The shells were then mixed with powder slurry and further

Fig. 4: Hull Rinser Assembly

Fig. 6: Vibratory Motor Mounting

Fig. 7: Rinsing Trials

Fig. 5: Helical Tray assembly with Inlet chute

more than 1200 operational trials were carried out. Various parameters like the current & voltage of motor, feed and discharge of hulls, operational time etc were recorded. Measurement of vibration in terms 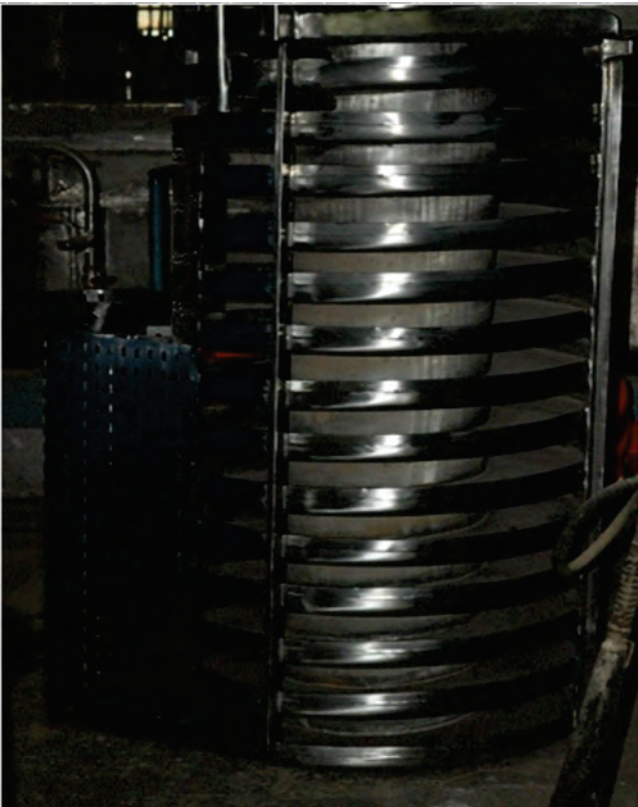of displacement, velocity and acceleration were also recorded. The reading was taken with empty tank and also tank filled with water with and without load.

Remote handling and maintenance is one of the concerns for any hot cell equipment. The components of the Hull Rinser which demands periodic maintenance, are made removable and provided with hooks at appropriate location. The hull rinser assembly has been designed for remote removal of drive assembly as well as the complete helical tray assembly. Dismantling and assembly of removable components were also satisfactorily carried out (Fig. 10).

Performance Evaluation and Observations

The trials with simulated hulls yielded desired results in terms of rinsing time and effectiveness of cleaning. It was observed that hulls weighing 7.5 kg (corresponding to hulls of 5 numbers of 220 MW PHWR Spent fuel) would be rinsed in 15 min time period. This gave sufficient time margin for next batch of rinsing as the CRD discharges hull after every one hour. Multiple number of trials were carried to maximum to verify and establish the time period.

weighed to estimated the quantity of the powder trapped on and within the shells. The shells are weighed again after the rinsing operation to determine the powder retained with the shells. 30 % of shells used in the trials were pinched at the ends to simulate the crimping due to shearing operation. The crimping prevents completed dissolution and tends to retain particulates within it. To check the reliability of components,
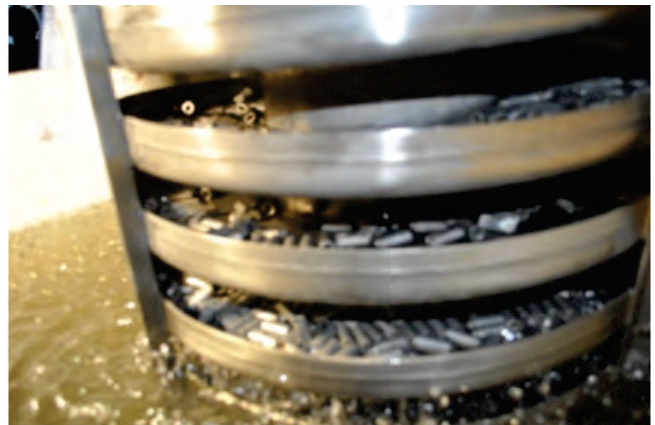
Fig. 8: Simulated hulls prior to rinsing

Fig. 9: Simulated hulls after rinsing

Rinsing trials were carried out on multiple occasions. On all occasions the effectiveness of rinsing operation was found satisfactory. Results of three such trials are indicated in Table 1.

Observation of parameters during the reliability trials for 1200 operations revealed consistency in results. The vibrating mass was observed to vibrate with an acceleration of 15-18g

Fig. 10: Handling Trials

with empty tank. The vibration however subsided to 10-12 g with filled tank. The addition of load (shells weighing 7.5 kg) didn't have any effect on vibration as it is insignificant compared to total vibrating mass. The support structure mounted on the floor was observed to vibrate with acceleration of 3-4 g . Similar acceleration was observed on tank surface also.

One significant observation was made during switching off the motor of equipment. As its rpm lowers from operation speed to zero it encounters resonance with the support frame resulting in large amplitude vibration for few seconds.

Table1: Rinsing trials

Trials	Shell weight (100 shells)	Shell + powder (wt)(Before Rinsing)	Powder (wt)	Shell + Powder (wt) (After rinsing)	% Removal	Remark
1	717.83 g	787.93 g	70.1 g	719.07 g	98. 23%	Mixed with wet powder
2	717.83 g	969.44 g	251.61 g	718.21 g	99.8%	Immersed in slurry
3	717.83 g	849.44 g	131.61 g	718.08 g	99.9%	Immersed in slurry and dried overnight

Further after multiple rinsing operation it was observed that dirt particles (accumulated after multiple operation) removed from the shell also tends to move along the helical path and discharge through the same route. Hence this called for some provision to avoid the same.

The shells also drag water droplets to the point of discharge and therefore a drying provision is essential.

Finite Element Analysis

In order to estimate the life expectancy and stress level of the component, vibration measurement and FE analysis were carried out by expert team of Vibration Lab, RED. Sensitive vibration probes (tri-axial-accelerometers) were mounted at different locations on the hull rinser and on supporting frame. Vibration data were acquired under various operating conditions. A finite element model was also prepared for analyzing the local stress levels and response to dynamic loading.

The stress observed at operating RPM (16.66 Hz) were well within the limits and gave infinite life for the components. The maximum stresses were however observed corresponding to the natural frequency of system (3.54Hz) encountered during coast down (i.e. stopping of Hull Rinser) at flange gusset which exceeded the endurance limit of the material. The same was resolved by increasing the gusset thickness which brought down the stress level well below endurance limit.

Conclusion

The Hull Rinser is first of a kind developmental effort which has yielded desired performance. The operation time, rinsing effectiveness and amenability to remote operation and maintenance make it suitable for automation of head end operation for a large throughput plant. Valuable feedback was obtained during manufacturing and trials of the industrial scale prototype which will aid in finalizing the design. Further, evaluation of life expectancy of components through experimental trials accompanied by theoretical modeling will aid in evolving a plant worthy equipment.

References

1. Shaji Karunakaran, D.A.S. Rao, K.N.S. Nair, "Development of novel Spent Fuel Chopper for PHWR Fuel", BARC Newsletter, P 35-38, Nov-Dec 2010.

2. Shaji Karunakaran, G. Sugilal, K.N.S. Nair, "Development of continuous rotary dissolver", BARC Internal Report, BARC/2012/I/023.

3. Shaji Karunakaran, G. Sugilal, S.S. Khan, K. Banerjee," Development of Centrifugal Clarifier for Feed Clarification in Reprocessing", BARC Internal Report , BARC/2015/I/027, P1-P26.

Development of Rotary Screw Calciner for Automation of Calcination Process

Shaji Karunakaran, G. Sugilal, K. Agarwal
Technology Development Division, NRG
Puneet Srivastava, K. Kumaraguru, J.S. Yadav
Fuel Reprocessing Division, NRG

Development of Rotary Screw Calciner (RSC) was initiated for calcination of heavy metal on continuous mode. The design of RSC was finalised considering the feedback obtained from past experience for ease of operation and maintenance as well as retrofitting of RSC inside active glove box. A compact design was evolved, manufactured and tested with surrogate material for performance evaluation. The system has been delivered to site for further inactive trials and implementation inside glove box.

Introduction

The solvent extraction process of fuel recycling consists of separation and purification of useful heavy metals. In subsequent process the heavy metals are converted back to oxide form. This process makes the product ready to be employed for fuel fabrication for next stage of fuel cycle facilitating the three stage nuclear program adopted by country for optimum use of natural resources for sustained energy requirement.

Reconversion Process

The heavy metals after solvent extraction process is in nitrate solution form. The final product in oxide form is obtained after following the stages of precipitation, filtration & calcination. The present mode of operation is semi continuous process. The precipitation of heavy metal in oxalate form in carried out in a precipitation column which is transferred to batch filter which employs sintered SS filter screen for removal of moisture. This cake is manually transferred to a boat which is placed inside a muffle furnace for calcination. The calcined product is manually transferred, blended and put in a can which is sealed out of glove box and stored in bird cage arrangement.

The criticality concern and extensive manual handling during multiple stages results in limiting the batch size. Further Man rem expenditure has also been a concern during operation and maintenance. For a large throughput plant this will result in multiple stream of production line and corresponding man power requirement. To address these concerns developmental efforts were initiated to switch over to continuous mode of process which reduces the human intervention. Development of continuous precipitation and rotary vacuum drum filter to automate the precipitation and filtration operation has already yielded encouraging results. Development of Rotary Screw Calciner was also initiated to automate the calcination process and compliment the equipment developed for continuous precipitation and filtration.

Calcination

This process involves conversion of oxalate of heavy metal into oxide under high temperature. Presently, it is achieved using a Muffle Furnace in which a container containing oxalate is kept for specified duration where it undergoes a heating cycle for drying and calcination. However, this involves manual handling of oxalate transfer to ignition boat, insertion of boat inside furnace and later removal of the boat from furnace followed by oxide transfer from the ignition boat. Since the heating elements are mounted on the furnace wall, sufficient residence time is required for oxalate powder in the interior (i.e. centre) to get converted. However, in this process the peripheral material is subjected to high temperature for more duration and this may result in varying product quality within the same batch. Blending operation follows calcination for proper mixing and uniformity of product.

Rotary Screw Calciner (RSC)

The calcination process can be achieved in continuous mode through Rotary Screw Calciner (RSC). The system consists of screw rotating in a long (tubular) furnace. The feed received at one end is pushed forward due to rotary action of the screw and discharged on the other end. The temperature of furnace is maintained such that the moisture in the feed gets removed through one-third length of furnace and subsequently undergoes calcination during the remaining two third length of high temperature zone of furnace.

Development of RSC has been undertaken earlier and unit based on tubular furnace (Fig. 1) with rotary screw and associated drive was manufactured (Fig.2). Multiple operational trials of unit were carried out under simulated conditions. However, the unit being larger in size was not found suitable for installation inside the existing glove box. Further, few modifications were also identified for improvement of operation and maintenance requirement.
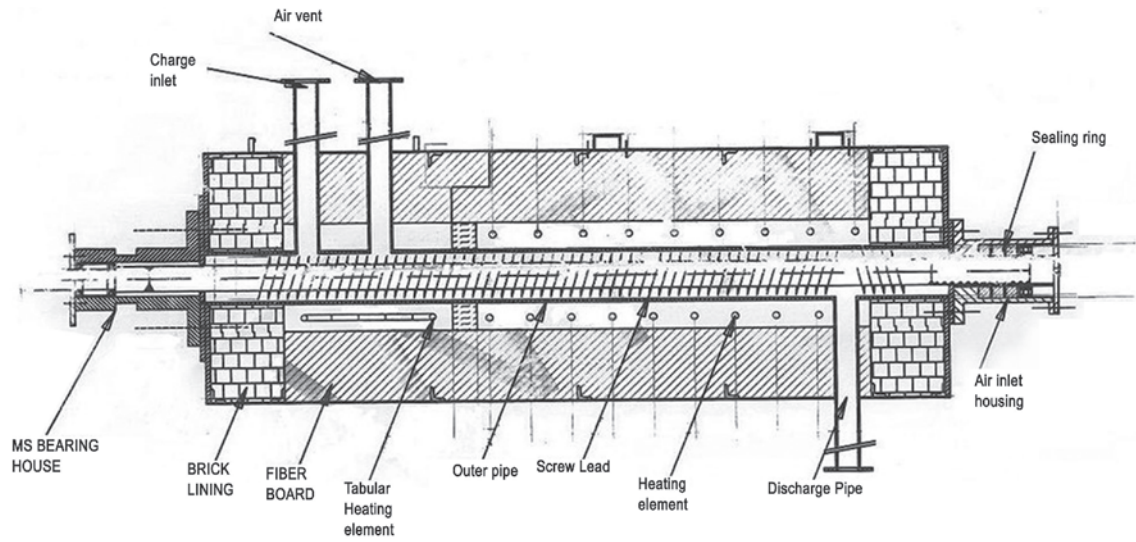
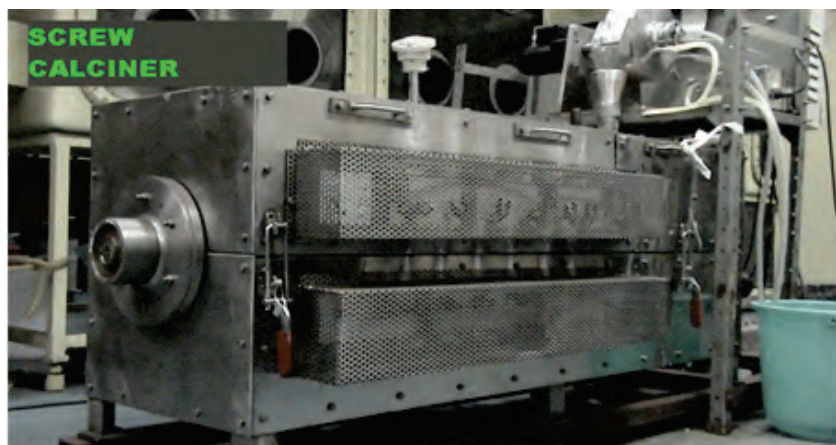**Fig. 1: Schematic of Tubular Rotary Screw Calciner**

Fig. 2: Engineering Scale Prototype of Existing Rotary Screw Calciner

Design Features

Since the objective was to retrofit the equipment in an existing active glove box, the sizing of equipment was done accordingly. The only access available in the existing glove box for installation of equipment is two square opening of 450mm x 450mm on the rear side along with access through glove ports from the front side. The RSC has therefore been designed to have a modular construction such that each module can be inserted inside the glove box through available opening on rear side and assembled through glove port from the front side (Fig. 3). The furnace construction was modified to "U" trough with hinged lid instead of earlier tubular design

to facilitate easy maintenance of screw and trough. The screw also has been designed as detachable unit which can be easily removed after opening the trough lid. The end shaft on either side of screw has been supported on ceramic bushes considering the operation speed and high temperature condition. The design of power transmission from drive motor to rotary screw through chain drive due to space constraint instead of direct mounting which would have increased the overall length of the assembly leaving no room for manoeuvring during maintenance activity. The furnace has also been designed for accommodating thermal expansion with floating support on one side. The furnace
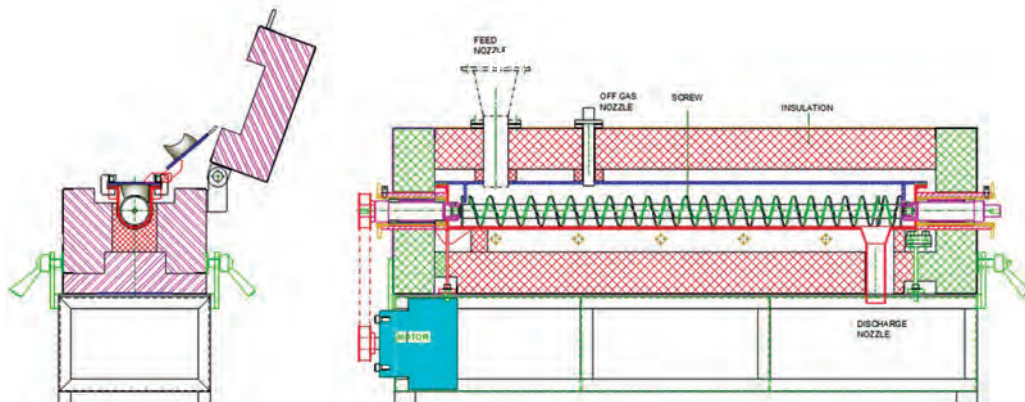

Fig. 3: Schematic of New Rotary Screw Calciner

insulation was also designed as modular panel which can be easily taken inside the glove box through the available opening and assembled inside the glove box. The furnace heating is achieved by rod type element of silicon carbide which can be easily removed and replaced in case of failure of any element.

Inconel 625 was selected as the material of construction for components handling metallic oxalate and experiencing high temperature, like the 'U' trough, screw, end shafts etc. All other components were fabricated out of SS 304 L material. Special Ceramic paper has been used as gasket material to maintain negative pressure inside the trough during operation. For insulation of the furnace, special grade microporous insulation have been used which has very low thermal conductivity as compared to conventional insulation material in order to design a compact unit suitable for existing glove box without compromising on final skin temperature.

Manufacturing

One of the critical requirements of RSC (Fig. 4) was to minimise the clearance between trough and screw(Fig. 5) to reduce the holding up of material. This demanded precision manufacturing of the trough and screw to achieve the desired results. The U trough was first formed out of Inconel plate after establishing its behaviour through multiple mock trials. Subsequently it was machined in horizontal boring machine to get the circular contour within desire tolerance at the bottom. The screw was fabricated out of multiple circular disc of Inconel formed into helical flight welded in series on machined shaft. The screw outer diameter was later machined to suit the internal circular contour of trough. The manufacture of insulation panel also has been a challenge with fragile nature of microporous insulation which disintegrated on any kind of penetration. It was finally sandwiched within

Fig. 4: Rotary Screw Calciner Assembly

Fig. 5: 'U' Trough and Screw

the fibre wool which gave it integrity while making holes for insertion of heating element and thermocouple. The insulation modules were fabricated with cover made of 2mm SS 304 sheets with hooks for handling during assembly and operation.

Controls and Instrumentation

The RSC is powered by Silicon Carbide heating element (Fig. 6) controlled by thyristor based compact PID controller based on thermocouples (K-Type) feedback. The rotary furnace is divided into two zones along the length, namely Drying Zone (maintained at 250°C) and Calcination Zone (maintained at 650°C). The zones are maintained by five heating elements of 1.5 kW each located at appropriate location with setting to suit the temperature requirement of zone.
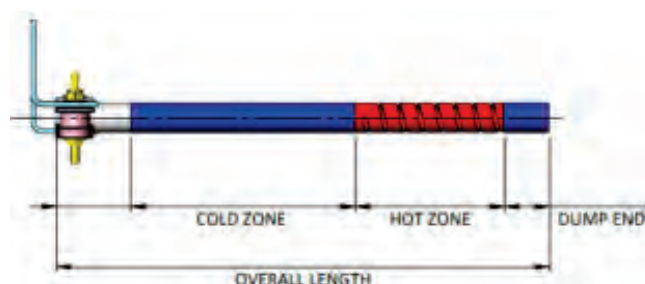

Fig. 6: Silicon Carbide Heater

Fig.7: Control Panel

The compact control panel (Fig. 7) is equipped with all required control switches and indicators like RYB phase indicator for incomer, 4-pole MCV (incomer), ammeter

(digital) for individual heating elements, individual heater control switch and thermocouple reading display etc.

The control panel is provided with a knob to control the rpm of helical screw. The speed is controlled through potentiometer with feedback from an inline encoder mounted on driving DC motor.

Experimental Trials

The manufactured prototype has undergone extensive trials to establish the intended design performance. These consisted of trials for establishing relation between screw rpm and residence time, repeatability of residence time for a given rpm, dummy heating trials without load and understanding heating element characteristics etc. After establishing necessary initial parameters, performance trial with surrogate material was carried out. Heating elements parameters were set appropriately to obtain well defined drying zone in one-third length and calcinations zone in remaining two-third. Thermocouple reading mounted at appropriate location gave

Fig. 8: Performance Trials

Fig. 9: Calcined Product

the temperature profile of drying as well as calcinations zone. Multiple trials (Fig. 8) were carried out with simulated feed at a rate of 0.5 kg/hr as well as 1 kg/hr. Temperature of the surface of the RSC was also continuously monitored using temperature gun. The calcined product (Fig. 9) was collected in container at the discharge end.

As mentioned earlier the design of RSC was carried out with objective of retrofitting it in an existing active glove box. To confirm the suitability of design for the same, a dummy glove box(Fig. 10) similar to the dimension of existing glove box was fabricated with similar opening. The complete installation procedure was simulated in dummy glove box (Fig. 11 A-D).

Fig. 10: Dummy Glove Box

Results and Observation

The initial trials carried out on RSC, established various operating parameters like the maximum residence time, effective zoning for drying and calcinations, desired calcinations temperature of 650 $^{\circ}$C, skin temperature of equipment within 50 $^{\circ}$C for protection of rubber gauntlet of glove port etc.

The performance trials with surrogate material yielded consistent results. The product obtained weighed equivalent to that of its oxide with a residence time of 50 min. The result is similar to what is obtained in calcination of actual heavy metal. Further, the holdup in the RSC after operation was observed was a nominal 25-30gm.

The assembly trials inside dummy glove box established the assembly sequence to be followed while installation in actual glove box. Minor modification in equipment for ease of installation was also carried out. The trials also established feasibility of handling any components within the glove box in case of maintenance.

(A)

(B)

(C)

(D)

Fig. 11(A-D) : Assembly of RSC inside Dummy Glove Box

Conclusions

The task of design, fabrication, assembly and testing of RSC for implementation in an active glove box has been a satisfactory experience albeit challenging. The design has considered the experience obtained from similar equipment manufactured earlier and improved upon for ease of operation and maintenance. The RSC has a significantly higher processing capacity as compare to the present plant requirement. The equipment after undergoing extensive trials at manufacturer's workshop has been delivered and presently installed in an inactive area for further trials. With the feedback obtained from operating plant the design can be scaled up to meet the requirement of future

Two Day joint NRG-BRNS National Seminar on Siting, Design and Safety Assessment of Radioactive Waste Disposal Facilities

Nuclear Recycle Group of Bhabha Atomic Research Centre organised the second National Seminar on "Numerical Methods in Site Characterisation, Design and Safety Assessment of Radioactive Waste Disposal Facilities" during 5-6 October 2017 in AERB. The major focus of the seminar was on Deep Geological Disposal System for ultimate disposal of vitrified long lived high-level radioactive wastes popularly known as Deep Geological Repositories (DGR). The main objectives of the national seminar included presentation of latest data and results of theoretical and experimental studies being taken up in NRG as well as under collaborative projects with national laboratories and institutes in this vital field of back end. The seminar also addressed technical aspects of impact of fission products separation, actinide partitioning and transmutation on Deep Geological Disposal System, requirement of Underground Research Laboratory, identification of new collaborative projects to support field scale experimentation related to waste disposal in DGR. The seminar comprised of two technical sessions including 21 talks by experts from NRG, NPCIL and collaborating national institutes. A total of 50 participants from BARC, NPCIL, AERB, Atomic Mineral Directorate for Exploration and Research (AMDER) etc attended the seminar. In addition to there form Indian Institute of Technology (IIT) Mumbai, Delhi, Patna, ISM Dhanbad, Indian Institute of Science (IISc) Bangalore, National Institute of Rock Mechanics (NIRM) Bengaluru, Delhi University (DU), and (AMDER) Hyderabad. Shri DK Shukla, Executive Director AERB was the chief guest of the inaugural function. Dr. R.K. Bajpai Head Repository Engineering Section and convener of the theme meeting in his welcome address gave a brief outline of the seminar and various topics covered. He also elaborated on international developments in this field in addition to various projects taken up in BARC. Dr. C.P. Kaushik CS WMD in his address elaborated on waste management practices in BARC

and also touched upon various new developments in the field of Cs pencil fabrication. He highlighted the need of DGR system to accommodate residual HLW that will be left after adaptation of separation technologies together with wide variety of other wastes that may eventually not qualify for shallow disposal.

Shri K. Agarwal, Associate Director, NRG in his address, highlighted the need of an Underground Research Station as an integral and essential step towards the implementation of Deep Geological Disposal programme in the back end of the fuel cycle. He explained the work going on in hill based waste disposal cum Underground Research Laboratory being operated by Korea. He emphasised on the importance of numerical methods in long term extrapolation of short duration experimental results and called for development of in house computer codes as well. Dr. B.S. Tomar Director, RC&IG highlighted the uniqueness of DGR project in terms of its very long time frames of safety and intense international effort being put in this vital field of back end especially in field of long term radionuclide migrations and sorption in various components of DGR. He dwelt upon ongoing collaborative research and development project between NRG and RC&IG.

Dr. D.K. Shukla stressed upon the complexity associated with implementation of DGR projects due to very long project duration and required safety periods. He further dwelt upon uncertainties associated with rock mass heterogeneity, excessively long time frames involved in safety assessment, limitation of experimental capability for long term demonstration of disposal system evolution. He also highlighted the need of developing safely guides and standards for such facilities. In technical sessions, an overview on the radioactive waste management and disposal in the Indian context was presented by Dr C.P. Kaushik, CS WMD. He stressed upon the fact that though the HLW inventory

Shri K. Agarwal AD, NRG delivering inaugural address

Shri D.K. Shukla Executive Director, AERB and chief guest of the National Seminar releasing abstract volume

Shri R K Bajpai Head RES, is delivering welcome address

Technical session is in progress

subsequent to adaptation of FP/ Actinide separation meant for disposal in deep geological system would reduce significantly, the residual HLW would still need to be disposed in deep geological systems in addition to waste like spent sources, alpha waste not qualifying for NSDF, long lived ILW etc. Dr R.K. Bajpai, presented an overview of the various plan and R&D projects so far carried out BARC for deep geological systems. He also elaborated the findings of Red Impact report jointly published by 21 European organisations on impact of partitioning and transmutation on deep geological disposal system. The report concludes that DGR remains indispensible, whatever procedures including P&T are adopted. It further concludes that such technology would only result in decreased size of the DGR without any appreciable impact on depth, siting requirements and doses from the facility.

The latest progress in the field of TMH response measurement and modelling on single over pack scale as well as complete DGR scale (2500 over packs), coupled TMH modelling of granite based Indian reference disposal system for hosting 10000 over packs, geotechnical, thermal, hydraulic and radiological data on Smectite clays of EBS, development of new in-house codes,TL dating application in site selection, radionuclide migration in NSDF facilities at Kota and Trombay etc are some of the important topics covered during

the seminar. Based on two days technical deliberations, intense discussions and a panel discussion, the need of DGR in Indian Nuclear Fuel Cycle was recognised as indispensible. Distinct need to set up Underground Research Facility at feasible site now and complete technology development and demonstration activity was also identified. It was observed that almost 27 such research facilities have been in operation worldwide in mines, hills and also as purpose built underground facilities. With Japan having developed two such underground facilities and also China with one hill based underground facility, it was recommended to focus efforts towards setting up similar low cost hill based facility in India. Other recommendations included initiation of a Coordinated Research Project (CRP) with BRNS funding as an umbrella project with 10 sub-projects to support proposed underground research station project in the field of pre-experimental modelling, sensor and probes development, Engineered Barrier Development, material performance in underground, rock mass parameter estimations etc and organisation of five refresher courses on rock mechanics, TMH modelling, glass& canister corrosion, Engineered Barrier System and NSDF at various collaborating institutes for the benefits of BARC, AERB and NPCIL young officers. It was also recommended to initiate development of safety guides and standards for DGR facilities in Indian context.

Training Course on "Basic Radiological Safety and Regulatory Measures for Nuclear Facilities", organised by BSC Secretariat

BSC Secretariat (BSCS) conducts many short-term training courses for the working personnel of BARC facilities, as part of its mandate towards enhancing safety culture. The thirty fourth course of this series "Basic Radiological Safety and Regulatory Measures for Nuclear Facilities" was conducted during October 25-28, 2017 at HPD Auditorium, CT&CRS Building, Anushaktinagar.

During the inauguration of the Course, Shri V. M. Jolly, Head, BSCS welcomed the participants. Shri K. Jayarajan, Chairman, BARC Safety Council (BSC) introduced the Course and explained its relevance. The Chief Guest, Shri H. Mishra, AD, ESG explained the necessity of adhering to regulatory codes, guides and procedures. Dr. D. Datta, Head, RP&AD emphasised on the radiological safety and radiation awareness during the keynote address.

The training course was carried out through classroom lectures, video displays and a visit to Dhruva reactor. It covered topics, such as regulatory framework of BARC, radiation basics and natural radiation, dosimetry and dose control, radiation detection and measurement; industrial safety, chemical safety, electrical safety, construction safety, occupational health, preparedness and response for nuclear and radiological emergencies, biological effects of radiation; regulatory inspections and event reporting. Faculties from BSCS, Radiological Physics & Advisory Division, Medical Division, Industrial Hygiene & Safety Section, Fire Services Section, Technical Services Division, Civil Engineering Division and Control & Instrumentation Division shared their knowledge and experience with the participants. Sixty-three participants attended the course.

During valedictory function, the Chief Guest Shri Y.K. Taly, former Chairman, BSC lauded the efforts of BSCS for its contribution towards improving safety awareness. The function was also graced by Dr. K. Madan Gopal, Associate Director, Materials Group and senior officers of BARC.

Shri V. M. Jolly, Shri K. Jayarajan, Shri H. Mishra and Dr. D. Datta during the release of compiled lecture notes

Participants, Faculties and Invitees during the Inagutation Session

Central Complex at BARC